Helping hand for melanoma invasion: transparent zebrafish can catch macrophages in the act

Neurochondrin interacts with the SMN protein suggesting a novel mechanism for Spinal Muscular Atrophy pathology.

Luke W Thompson[1], Kim D Morrison[1], Sally L Shirran[1], Ewout JN Groen[2], Tom H Gillingwater[2], Catherine H Botting[1], Judith E Sleeman[1], 1.University of St Andrews, School of Biology, BSRC Complex, North Haugh St Andrews, KY16 9ST, UK. 2. Edinburgh Medical School: Biomedical Sciences and Euan MacDonald Centre for Motor Neuron Disease Research, University of Edinburgh, Hugh Robson Building, George Square, Edinburgh, EH8 9XD, UK.

jes14@st-andrews.ac.uk

Key Words: Spinal Muscular Atrophy, Neurochondrin, SMN, Sm Proteins, snRNPs

JCS Advance Online Article. Posted on 5 March 2018

Summary Statement

The essential neural protein neurochondrin interacts with the Spinal Muscular Atrophy (SMA) protein, SMN, in cell lines and in vivo. This may be relevant to the molecular pathology of SMA.

Abstract

Spinal Muscular Atrophy (SMA) is an inherited neurodegenerative condition caused by reduction in functional Survival Motor Neurones Protein (SMN). SMN has been implicated in transport of mRNA in neural cells for local translation. We previously identified microtubule-dependant mobile vesicles rich in SMN and SmB, a member of the Sm family of snRNP-associated proteins, in neural cells. By comparing the interactomes of SmB and SmN, a neural-specific Sm protein, we now show that the essential neural protein neurochondrin (NCDN) interacts with Sm proteins and SMN in the context of mobile vesicles in neurites. NCDN has roles in protein localisation in neural cells, and in maintenance of cell polarity. NCDN is required for the correct localisation of SMN, suggesting they may both be required for formation and transport of trafficking vesicles. NCDN may have potential as a therapeutic target for SMA together with, or in place of, those targeting SMN expression.

Introduction

The inherited neurodegenerative disease, Spinal Muscular Atrophy (SMA) is caused by a reduction in the amount of functional Survival Motor Neuron (SMN) protein (Lefebvre et al., 1995). SMA is the leading genetic cause of infant mortality, affecting 1:6000 live births (Monani, 2005). The recently developed therapy, Spinraza/Nusinersen (Biogen) has been shown to increase the level of SMN and improve the symptoms of SMA patients (Corey, 2017; Finkel et al., 2016; Passini et al., 2011). Most SMA patients harbour mutations in the SMN1 gene, which produces the majority of total SMN protein in cells. In humans, expression from a variable number of copies of an additional gene, SMN2, can produce some full-length SMN protein (Lefebvre et al., 1995; Lefebvre et al., 1997). The SMN2 gene, unlike SMN1, contains a point mutation in an exon splicing enhancer (Lorson and Androphy, 2000; Lorson et al., 1999) resulting in truncation of most of the SMN protein produced by SMN2 through skipping of exon 7. The truncated protein produced by SMN2 is less stable than full-length SMN and cannot compensate fully for the loss of SMN1 (Le et al., 2005; Lorson and Androphy, 2000; Lorson et al., 1999). However, due to the small amounts of full length SMN expressed from the SMN2 gene, the number of gene copies can influence the severity of SMA, with evidence that five copies of SMN2 may be enough to compensate for loss of SMN1 (Campbell et al., 1997; Prior et al., 2004). It is not currently clear how a deficiency of functional SMN leads to the specific symptoms of SMA. In particular, the differing sensitivity of cell

types to lowered SMN levels, with motor neurons (MNs) most severely affected, is difficult to explain as SMN is an essential protein and complete deletion is lethal at the cellular level (Hsieh-Li et al., 2000; Schrank et al., 1997).

SMN localises to nuclear Cajal bodies and gems (Gemini of Cajal bodies (CBs)) (Liu and Dreyfuss, 1996) as well as in the cytoplasm and is implicated in a growing number of cellular roles in both locations (Hosseinibarkooie et al., 2017; Li et al., 2014; Monani, 2005; Singh et al., 2017; Sleeman, 2013; Tisdale and Pellizzoni, 2015). The first to be elucidated was a role in the early, cytoplasmic, stages of assembly and maturation of splicing snRNPs (small nuclear ribonucleoproteins). Splicing snRNPs are ribonucleoprotein complexes, essential for pre-mRNA splicing, comprising an snRNA (small nuclear RNA) core and numerous proteins including a heptameric ring containing one copy each of members of the Sm protein family. SMN is part of a cytoplasmic complex, also containing the gemin proteins, required for the addition of the Sm proteins as a ring around the snRNA core (Li et al., 2014; Liu et al., 1997; Stark et al., 2001; Tisdale and Pellizzoni, 2015). The maturation of snRNPs has been shown to be impaired by a deletion in SMN (Gabanella et al., 2007; Shpargel and Matera, 2005; Wan et al., 2005; Winkler et al., 2005; Zhang et al., 2008), while alterations to pre-mRNA splicing events, proposed to be a downstream consequence of this impairment, have been observed in several models of SMA (Custer et al., 2013; Huo et al., 2014; Zhang et al., 2008). One of the proposed mechanisms for the cell-type specificity of SMA is that these alterations of pre-mRNA splicing events affect mRNA transcripts that are essential for motor neurons, perhaps preferentially affecting transcripts spliced by the minor spliceosome (Boulisfane et al., 2011; Custer et al., 2016; Doktor et al., 2017; Gabanella et al., 2007; Zhang et al., 2008). Despite promising results in Drosophila models, however, specific transcripts affecting MNs are yet to be conclusively identified (Lotti et al., 2012).

Another well-established cellular role of SMN is in the trafficking of mature mRNA within the cytoplasm, particularly in the axons and neurites of neural cell types. (Akten et al., 2011; Custer et al., 2013; Fallini et al., 2016; Fallini et al., 2014; Fallini et al., 2011; Li et al., 2015; Lotti et al., 2012; Peter et al., 2011; Rossoll et al., 2003; Rossoll et al., 2002; Todd et al., 2010a; Todd et al., 2010b; Zhang et al., 2006; Zhang et al., 2003). This is thought to be linked to local translation of mRNA into proteins, an important process for neural cells, in particular motor neurones, due to the length of their axons (Doyle and Kiebler, 2011; Holt and Schuman, 2013; Huber et al., 2000; Kang and Schuman, 1996), making this trafficking role for SMN of particular interest for

understanding the cellular pathology of SMA. SMN co-localises with the mRNA binding proteins HuD, IMP1 and hnRNP R and is involved in the localisation of mRNAs to axons (Akten et al., 2011; Fallini et al., 2014; Fallini et al., 2011; Rossoll et al., 2003). The cellular structures involved in SMN-dependent mRNA trafficking are currently unclear, being described as granular (Akten et al., 2011; Fallini et al., 2014; Peter et al., 2011; Todd et al., 2010b; Zhang et al., 2006; Zhang et al., 2003) or vesicular in nature (Custer et al., 2013; Prescott et al., 2014).

SMN has also been implicated in many other processes. Some of these involve a role in RNP assembly, similar to the canonical role in splicing snRNP production, including assembly of both the signal recognition particle and the U7 snRNP required for 3' processing of histone mRNA (Azzouz et al., 2005; Piazzon et al., 2013; Tisdale et al., 2013). Other roles are more diverse and include the regulation of cytoskeletal dynamics and endocytosis (Bowerman et al., 2007; Dimitriadi et al., 2016; Giesemann et al., 1999; Hao le et al., 2012; Heesen et al., 2016; Hosseinibarkooie et al., 2016; Nolle et al., 2011; Oprea et al., 2008; Riessland et al., 2017); enhancement of DNA repair (Takaku et al., 2011); transcriptional regulation (Pellizzoni et al., 2001; Zhao et al., 2016; Zou et al., 2004); stress granule formation (Hua and Zhou, 2004; Zou et al., 2011) and ubiquitin homeostasis (Wishart et al., 2014). It is currently unclear whether or how disruption of the many proposed roles for SMN contributes to SMA pathogenesis.

Structures containing the SMN and SmB proteins, alongside Coatomer Gamma are trafficked on microtubules (Prescott et al., 2014). Evidence suggesting that SMN/SmB-rich structures are vesicular in nature includes their staining with lipophilic dyes in living neural cells, their vesicular appearance using correlative fluorescence and electron microscopy (Prescott et al., 2014), and the interaction of SMN and the Sm proteins with Coatomer proteins, which are associated with membrane bound vesicles (Custer et al., 2013; Peter et al., 2011; Prescott et al., 2014). We have previously identified an interaction between SmB and dynein cytoplasmic 1 heavy chain 1 (DYNC1H1), a motor protein required for microtubule transport (Prescott et al., 2014), mutation in which can cause a rare, lower extremity dominant SMA (Chen et al., 2017; Ding et al., 2016; Harms et al., 2010; Harms et al., 2012; Niu et al., 2015; Peeters et al., 2015; Punetha et al., 2015; Scoto et al., 2015; Strickland et al., 2015; Tsurusaki et al., 2012). SMN has also been shown to associate with the membranous Golgi complex (Ting et al., 2012), while mutations in the Golgi-related protein BICD2 (bicaudal D homolog 2) cause a form of lower extremity dominant SMA (Martinez-Carrera and Wirth, 2015; Neveling et al., 2013; Oates et al., 2013; Peeters et al., 2013; Rossor et al., 2015; Synofzik et al., 2014).

The Sm protein family is implicated in both of the major functions of SMN. The core of splicing snRNPs comprises a heptameric ring of proteins around the snRNA, containing SmB/B', D1, D2, D3 E, F and G (Urlaub et al., 2001). SMN is a vital part of the complex required for the assembly of this Sm protein ring (Battle et al., 2006; Fischer et al., 2011; Fischer et al., 1997; Liu and Dreyfuss, 1996; Meister et al., 2001; Meister and Fischer, 2002; Pellizzoni et al., 2002). Other members of the Sm protein family have also been identified, beyond the core proteins usually found in splicing snRNPs. Of particular interest in the context of SMA pathology is SmN (encoded by the SNRPN gene), which is expressed in neural tissues (Schmauss et al., 1992) and can replace SmB in the heptameric Sm protein ring (Huntriss et al., 1993). The human SmN protein differs from SmB' by 17 amino acids (UniProt Identifiers P63162 and P14678 respectively), and little is known about its behaviour other than its incorporation into snRNPs, although the SNRPN gene locus is within the paternally imprinted region of the genome critical in Prader-Willi Syndrome (Ozcelik et al., 1992). There is growing appreciation that some Sm proteins may 'moonlight' in functions beyond their presence in splicing snRNPs. In addition to the role of SmB in cytoplasmic trafficking vesicles in human cells, in Drosophila SmB and SmD3 are implicated in mRNA localisation (Gonsalvez et al., 2010) and SmD1 has a role in miRNA biogenesis (Xiong et al., 2015). With this in mind, we applied a proteomic approach in the neural cell line SH-SY5Y to search for interactions that could indicate neural specific roles for the SmN protein of relevance for the pathology of SMA.

This proteomic approach led to the identification of Neurochondrin (NCDN) as a novel interactor of both SmN and SMN. NCDN is an essential protein predominantly expressed in neural tissue and involved in neural outgrowth, synaptic plasticity and moderation of signal transduction (Dateki et al., 2005; Francke et al., 2006; Matosin et al., 2015; Pan et al., 2016; Shinozaki et al., 1999; Shinozaki et al., 1997; Wang et al., 2013; Wang et al., 2009; Ward et al., 2009). Further investigation of the relationship between NCDN and SMN suggest that NCDN interacts with SMN in the context of mobile cytoplasmic vesicles containing SmB and SmN and is strongly expressed in motor neurones. This suggests that NCDN warrants further investigation in the context of SMA pathology and may proves useful as a target for future therapy development.

Results

SmN exhibits similar behaviour to SmB, localising to cytoplasmic vesicles containing SMN

In order to determine the interactome of the neural-specific Sm protein, SmN, we first generated constructs to express fluorescent protein-tagged SmN by amplifying the SmN sequence from total RNA from SH-SY5Y cells and cloning it into the pEYFP-C1 and pmCherry-C1vectors. All of the Sm fusion proteins studied so far show a steady-state localisation to nuclear Cajal Bodies (CBs) and speckles. The Sm proteins SmB, SmD1 and SmE have also previously been shown to exhibit a characteristic pathway within the cell on their initial expression, indicative of the snRNP maturation pathway (Sleeman and Lamond, 1999), although differences were seen between the Sm proteins. To confirm that YFP-SmN localised correctly at steady state to CBs and speckles, and to determine where SmN localised during maturation and incorporation into snRNPs, the plasmid was transiently expressed in SH-SY5Y neuroblastoma cells, with cells fixed and immunostained at 24 hour intervals. At 48 and 72 hours after transfection, YFP-SmN predominantly localised to speckles and Cajal bodies (CBs, detected with anti-coilin) identically to endogenous Sm proteins (detected with Y12 antibody), whereas at 24 hours, YFP-SmN localised predominantly diffusely within the cytoplasm, with some accumulation in CBs (Fig 1A, B). This sequential localisation is indistinguishable from that previously observed with YFP-SmB in HeLa and MCF-7 cells, though CBs were not prominent in the majority of SH-SY5Y cells transiently expressing YFP-SmN. Equivalent results were obtained in SH-SY5Y cells transiently expressing mCherry-SmN (Fig S1). Both YFP-SmN and mCherry-SmN are efficiently incorporated into splicing snRNPs, as evidenced by their enrichment from whole-cell lysates using antibodies against the characteristic hypermethylated Cap structure (2,2,7-trimethylaguanosine) found on snRNAs (Fig 1C).

To determine whether the similarities between SmN and SmB extend to localisation in detergent-sensitive vesicles in the cytoplasm (Prescott et al., 2014), SH-SY5Y cells constitutively expressing mCherry-SmN were used for live-cell time-lapse microscopy. Mobile mCherry-SmN foci were observed (movie S1). In common with the SmB vesicles, these stained positive with the lipophilic dye, BODIPY 493, indicating that they are vesicular in nature (Fig 1D). Finally, to confirm

that the mCherry-SmN vesicles were similar to those previously identified with SmB, SH-SY5Y cells constitutively expressing mCherry-SmN were transfected with plasmids to express either GFP-SMN or YFP alone. GFP-SMN co-localised with mCherry-SmN in 83% (±11) of SmN-positive vesicles, which is statistically significant when compared to 8.4% (±4.5) of mCherry-SmN vesicles co-localising with YFP alone (Fig 1E, F).

Mass Spectrometry reveals similarities between the interactomes of SmN and SmB

As SmN appeared to behave very similarly to SmB in neural cells, it was unclear why neural cells express two almost identical proteins. It was decided to investigate whether SmN and SmB may have differing roles that could be identified by proteomic analysis. SH-SY5Y cells were selected for this analysis as they are easy to culture and amenable to the generation of cell lines constitutively expressing FP-tagged proteins, while retaining neural characteristics including the expression of neural proteins. They are also human in origin. Proteins interacting with YFP-SmB and YFP-SmN were affinity purified using GFP-TRAP (Chromotek) from whole-cell lysates of SH-SY5Y cell lines constitutively expressing the tagged proteins, with a cell line expressing YFP alone as a control for non-specific binding to the tag or bead matrix. Immunoblot analysis using antibodies to YFP demonstrated that the enrichment of the tagged proteins was 20X, 23X and 4X for YFP-SmN, YFP-SmB and YFP alone respectively (Fig 2A). The affinity purified material was size separated using SDS-PAGE and analysed by nLC ESI MS/MS mass spectrometry to identify peptides and therefore proteins interacting with YFP-SmB and YFP-SmN. Following removal of likely contaminants identified by their interaction with YFP alone, or their previous identification as common interactors of GFP-TRAP (Trinkle-Mulcahy et al., 2008), UniProt Biological Process and Cellular Component Genome Ontology annotations were used to group identified proteins into categories depending on function. These groups were then used to determine whether there were differences in possible functions between SmN and SmB (Fig 2B). Numerous proteins previously established to interact with Sm proteins were identified including SMN and the gemins as well as the methylosome components PRMT5, MEP50 and pICln, validating our approach (Table S2). The overall proportions of proteins in each category were similar when comparing the interactomes of SmN to SmB, though differences were identified at the level of individual proteins. Of particular interest in the context of SMA were a number of proteins with potential neural specific roles, which were identified in one or both samples. One of these was Neurochondrin (NCDN), a

relatively poorly characterised neural protein, which was identified in the YFP-SmN interactome, with 5 unique peptides identified (Fig 2D).

Neurochondrin interacts with SmN, SmB and SMN in cell lines and in vivo

To verify the interaction between Sm proteins and Neurochondrin, a construct expressing NCDN-GFP was generated. Affinity purification of NCDN-GFP from whole cell lysates of SH-SY5Y cells transiently co-expressing NCDN-GFP and mCherry-SmB demonstrated interaction between NCDN-GFP and mCherry-SmB (Fig 3A). To further investigate interactions between NCDN and the Sm proteins neural cells, an SH-SY5Y cell line constitutively expressing NCDN-GFP was established. Affinity purification of NCDN-GFP from whole cell lysates followed by immunoblot analysis using antibodies against endogenous SmN and SmB (Fig 3B) revealed that NCDN-GFP interacts with both SmN and SmB. Furthermore, both endogenous SMN and endogenous βCOP (a coatomer vesicle protein) were also revealed to interact with NCDN-GFP, suggesting that NCDN interacts with the Sm proteins and SMN in the context of cytoplasmic vesicles. Affinity purification of YFP alone from whole cell lysates of an SH-SY5Y cell line constitutively expressing YFP does not result in co-purification of endogenous SMN, SmB or βCOP (Fig 3C). To further investigate the interaction between SMN and NCDN observed in Fig 3B, a reciprocal experiment was performed using GFP-Trap to affinity purify GFP-SMN from an SH-SY5Y cell line constitutively expressing GFP-SMN (Clelland et al., 2009). Subsequent immunoblot analysis using antibodies to endogenous NCDN demonstrated that NCDN co-enriched with GFP-SMN (Fig 3D). To determine whether this interaction also occurs between the endogenous proteins at normal expression levels, we first immuno-precipitated endogenous SMN from whole cell lysates of SH-SY5Y cells. Immunoblot analysis using antibodies to endogenous NCDN (Fig 3D) confirmed that endogenous SMN interacts with endogenous NCDN. Moreover, to determine whether this interaction is also present at endogenous levels *in vivo*, and thus of potential relevance to SMA pathology, SMN was immuno-precipitated from lysates of P8 mouse brain. Again, we confirmed that endogenous SMN interacts with endogenous NCDN *in vivo* (Fig 3E). Together, these results confirm the interaction of SMN and NCDN at endogenous levels and *in vivo*.

Neurochondrin co-localises with SmN, SmB and SMN in cytoplasmic vesicles but not nuclear foci and is strongly expressed in motor neurones in mouse spinal cord.

To determine the probable cellular location for the interaction between SmN/SmB and NCDN, plasmids to express either NCDN-GFP or YFP were transiently transfected into SH-SY5Y cells constitutively expressing mCherry-SmN. This revealed that NCDN-GFP, but not YFP alone, accumulates in cytoplasmic vesicles containing mCherry-SmN (Fig 4A). Similar results were obtained when NCDN-GFP was transiently expressed in SH-SY5Y cells constitutively expressing mCherry-SmB (Fig S3). To investigate the probable cellular location of interactions between SMN and NCDN, mCherry-SMN was co-expressed with either NCDN-GFP or YFP alone. NCDN-GFP was found in cytoplasmic structures enriched in mCherry-SMN (Fig 4B). These data suggest that NCDN co-localises with both the Sm proteins and SMN in cytoplasmic vesicles, although NCDN-GFP shows an increase diffuse signal compared to the Sm proteins or SMN. Within the nucleus, antibodies to endogenous NCDN showed very little nuclear staining, with nuclear foci evident in very few cells (≤2%). These foci did not stain with antibodies to either coilin or SMN (Fig 4C) indicating that they are neither Cajal bodies nor gems. In sections from murine P5 spinal cord (Fig 4D,E), NCDN shows robust expression throughout the spinal cord. Interestingly, NCDN was most prominently expressed in ChAT-positive motor neurons in the ventral horn of the spinal cord (arrows in Fig 4D, enlarged in Fig 4E). This indicates that NCDN is enriched in motor neurons: the most relevant cell type for SMA.

NCDN, SMN and Sm protein co-fractionate with coatomer proteins.

To further investigate the possibility that the interaction of NCDN with SMN and the Sm proteins occurs within cytoplasmic vesicles, sub-cellular fractionations were performed on both parental SH-SY5Y cells and SH-SY5Y cell lines constitutively expressing NCDN-GFP, YFP-SmB, YFP-SmN or YFP. Sequential centrifugation was used to separate the cells into a nuclear fraction, 16,000 RCF and 100,000 RCF cytoplasmic pellets and cytosolic supernatant (De Duve, 1971). Immunoblotting of these sub-cellular fractions revealed that GFP-NCDN, YFP-SmB and YFP-SmN,

were all enriched in the 100,000 RCF cytoplasmic pellet, along with endogenous SMN and coatomer proteins (Fig 5). This fraction would be expected to contain membrane-bound structures, such as microsomes and small cytoplasmic vesicles, which would encompass small coatomer type endocytic vesicles. Endogenous SmN was also observed to enrich similarly (Fig S4). NCDN-GFP shows a larger proportion of protein in the remaining cytosolic supernatant when compared to YFP-SmB, YFP-SmN and endogenous SMN, which is in agreement with the sub-cellular localisations observed (Fig 4). This further supports our hypothesis that the interactions between NCDN, SMN and the Sm proteins take place in small cytoplasmic vesicles.

NCDN is required for the correct sub-cellular localisation of SMN

We have previously documented that reduction of SmB expression results in re-localisation of SMN into numerous nuclear structures, probably analogous to gems (Gemini of CBs), and its loss from cytoplasmic structures (Prescott et al., 2014). To investigate the requirement for NCDN in cytoplasmic SMN localisation, an SH-SY5Y cell line constitutively expressing GFP-SMN (Clelland et al., 2009) was transfected with siRNAs targeting NCDN (4 different single siRNAs (Dharmacon) and a pooled sample). A reduction in NCDN expression caused an increase in the number of SMN-positive nuclear foci present in the cell nucleus, as did a reduction of SmB expression (Fig 6A, B). Conversely, reduction in SMN expression reduced the number of SMN-positive nuclear foci. The use of non-targeting control (siControl) sequences or positive control siRNAs (targeting Lamin A/C) had no effect on the number of SMN-positive nuclear foci. The reduction in gene expression, assayed by immunoblotting, for each siRNA was typically 40-60% (Fig 6C). This suggests that NCDN is required for the correct sub-localisation of SMN. Of potential relevance for SMA pathology, depletion of either NCDN or SmB causes GFP-SMN to adopt a sub-cellular localisation reminiscent of that shown by GFP-SMNΔ7 (Fig 6), a truncated version of SMN that mimics the product of the SMN2 gene and is unable to completely substitute for full-length SMN in models of SMA (Le et al., 2005; Monani et al., 1999; Monani et al., 2000).

SMN is required for the correct sub-cellular localisation of NCDN

To investigate whether NCDN requires the SMN protein for its localisation to vesicles in neural cells, SH-SY5Y cells were transfected with shRNA constructs previously validated to reduce the expression of SMN by an average of 46%, a reduction previously found to cause symptoms resembling SMA Type III in mouse models (Jablonka et al., 2000), and carrying a GFP marker to unequivocally identify transfected cells (Clelland et al., 2012). Reduction of SMN, monitored by quantitation of the number of SMN-positive nuclear foci (Fig 7A,C), reduced the number of cytoplasmic foci containing endogenous NCDN (Fig 7A, B). This, together with data in Figure 6, suggests that NCDN and SMN are mutually dependent for their incorporation into cytoplasmic structures, raising the possibility that the lowered levels of SMN seen in SMA could compromise NCDN function.

NCDN does not co-purify with splicing snRNPs, suggesting it is not involved in snRNP assembly

To investigate whether the interaction between NCDN and SMN could reflect a previously unidentified role for NCDN in snRNP assembly, splicing snRNPs were affinity purified from whole cells lysates of SH-SY5Y cells constitutively expressing NCDN-GFP using agarose beads coupled to antibodies against the characteristic tri-methyl guanosine Cap of snRNAs (TMG beads, Millipore) (Fig 8A). Endogenous SmN protein showed strong enrichment in the affinity purified snRNP samples, as expected for a core snRNP protein. Endogenous SMN was also co-enriched with snRNPs, demonstrating that the experimental conditions were suitable to identify proteins important for snRNP assembly as well as those that are genuine snRNP components. NCDN-GFP did not co-purify with splicing snRNPs, however, suggesting that NCDN is not involved in snRNP assembly or processing. This raises the intriguing possibility that the interaction between SMN and NCDN reflects a novel, snRNP-independent role for SMN.

SMN interacts with Rab5 in SH-SY5Y cells and co-localises with a sub-set of Rab5 vesicles.

Recent studies have found that SMA may cause endocytic defects, especially in synaptic vesicle recycling in animal models (Dimitriadi et al., 2016). Several SMA-protective disease modifier genes, such as Plastin 3, Coronin 1C, and Neurocalcin Delta, are also associated with endocytosis (Hosseinibarkooie et al., 2016; Oprea et al., 2008; Riessland et al., 2017). However, other endocytic structures within the cell have not been investigated. Rab5 is a marker of early endosomes and endocytic vesicles, as well as being a regulator of these trafficking pathways (Bucci et al., 1992). NCDN and Rab5 have previously been shown to interact, while both Rab5 and NCDN both have roles in dendrite morphogenesis and cell polarity (Guo et al., 2016; Oku et al., 2013; Satoh et al., 2008).

As we had previously shown that SMN and NCDN co-localise in vesicles, we hypothesised that some of the SMN-rich vesicles could be Rab5 vesicles. SH-SY5Y cells were co-transfected with plasmids to express mRFP-Rab5 (Vonderheit and Helenius, 2005) together with either GFP-SMN, NCDN-GFP or YFP. mRFP-Rab5 was affinity-purified from whole cell lysates from each co-transfection using RFP-TRAP (Chromotek). Subsequent immunoblotting revealed co-purification of GFP-SMN and NCDN-GFP, but not YFP alone, with mRFP-Rab5 (Fig 8B). Furthermore, endogenous SMN also co-purified with mRFP-Rab5. In parallel experiments, co-localisation of mRFP-Rab5 with GFP-SMN and NCDN was investigated (Fig 8C,D). In accordance with previous publications, Rab5 showed partial co-localisation with NCDN-GFP in cytoplasmic structures (arrows in Fig 8D) (Oku et al., 2013). GFP-SMN showed a similar degree of co-localisation with mRFP-Rab5, also in cytoplasmic structures, while there was minimal co-localisation between YFP and mRFP-Rab5. Taken together with the absence of NCDN from enriched snRNP fractions (Fig 8A), this suggests that NCDN and SMN co-localise in the context of Rab5 vesicles, independently of snRNP assembly.

Discussion

The genetic cause of SMA has been known since 1995 (Lefebvre et al., 1995), but there is still little available in the way of treatment. Spinraza/Nusinersen is now available to treat SMA by correcting the defective splicing of the SMN2 transcript to promote production of full-length SMN protein. However, this is not a complete cure and requires regular maintenance doses through intrathecal injection. Additionally, little has been done to investigate potential symptoms that could arise later in life or in other tissues and organs in patients treated with Spinraza. Additional treatment options for SMA are still needed, for use in addition to Spinraza, or in place of it for patients for whom it is not suitable, including those with rarer forms of SMA in which SMN is not mutated.

A significant reason for the lack of treatment options for SMA is uncertainty about the cellular roles of SMN, which appear to be numerous. In particular, it is not clear why motor neurones are so exquisitely sensitive to reduced levels of SMN when the key roles of the protein appear to be in pathways required in all cell types. By comparing the interactomes of two very similar members of Sm protein family, SmB and the neural-specific SmN, we have uncovered an interaction between SMN and the essential neural protein NCDN, which may be of relevance for SMA pathology and have the potential to open novel avenues for therapy development.

The neural-specific Sm protein, SmN, behaves similarly to SmB, but shows subtle differences at the interactome level that may indicate alternative roles.

Differences between members of the Sm protein family have not been systematically investigated, although non-splicing roles have been proposed for SmB and SmD3 in mRNA localisation and for SmD1 in miRNA biogenesis in Drosophila (Gonsalvez et al., 2010; Xiong et al., 2015). As SmB and SmN are thought to perform the same primary function in snRNPs (Huntriss et al., 1993), it is currently unknown why SmN is expressed in neural tissues as well as, or instead of, SmB. Current research has suggested that the expression of SmN may cause tissue specific alternative splicing of pre-mRNA transcripts (Lee et al., 2014). However, an alternative, but complimentary hypothesis is that SmN may be adapted for secondary, neural specific roles. We

demonstrate here that SmN localises identically to SmB during snRNP maturation and at steady-state, when both localise to vesicles containing SMN in the cytoplasm and neurites of SH-SY5Y cells in addition to their canonical localisation to nuclear CBs and speckles. Our parallel proteomic study used SH-SY5Y neural cell lines constitutively expressing YFP-SmN and YFP-SmB to investigate difference between the interactomes of these two, very similar, proteins. SmN has a proline rich C-terminal tail that SmB lacks, although a similar sequence is present in SmB' (Mourao et al., 2016), an alternatively-spliced product of the SNRPB gene, which encodes SmB. Several proteins were identified in the SmN interactome but not the SmB interactome such as nuclear receptor co-activator 6 interacting protein (UniProt Q96RS0), and 7SK snRNA methylphosphate capping enzyme (UniProt Q7L2J0), both of which are associated with snRNA capping (Hausmann et al., 2008; Jeronimo et al., 2007). Additionally, RNA-binding protein 40 (UniProt Q96LT9) was uniquely identified within the SmN interactome, and is involved in the minor spliceosome (Benecke et al., 2005). This suggests that some of these proteins may interact preferentially with SmN, perhaps mediated by amino acid changes within the proline-rich tail. However, further validation and additional experimentation would be required to confirm these differences in interactome between SmN and SmB and to investigate specific functions for the distinct Sm protein family members.

NCDN interacts with SMN, SmB and SmN and co-localises with them in vesicles, suggesting a novel cellular role for SMN.

Previous research into neural-specific functions for SMN has identified several new protein-protein interactions involving SMN. These novel SMN partners have, in the main, been RNA binding proteins (Akten et al., 2011; Fallini et al., 2014; Fallini et al., 2011; Rossoll et al., 2003). There is growing appreciation that SMN-mediated transport may be of particular importance in neural cells and involve COP1-type vesicles transported by Dynein and containing SmB (Custer et al., 2013; Li et al., 2015; Peter et al., 2011; Prescott et al., 2014). The nature and content of these vesicles is not clear but they are likely to be of significance for the cell-type bias of SMA symptoms, as they are present predominantly in neural cells (Akten et al., 2011; Fallini et al., 2016; Fallini et al., 2014; Fallini et al., 2011; Li et al., 2015; Peter et al., 2011; Prescott et al., 2014; Rossoll et al., 2003; Todd et al., 2010a; Todd et al., 2010b; Zhang et al., 2006; Zhang et al.,

2003). The SmN/SmB interactome screen presented here suggests a large number of non-snRNP proteins as potential cellular partners for the Sm proteins.

We chose to investigate the neural protein NCDN further, as it has characteristics that may be of relevance for SMA. NCDN is predominantly expressed in neural tissue, and little is known about its structure or function, as it shares little sequence homology with other eukaryotic proteins (Shinozaki et al, 1997). Though characterised relatively poorly, it is associated with dendrite morphogenesis and localises to Rab5 vesicles involved in the maintenance of cell polarity (Guo et al., 2016; Oku et al., 2013), NCDN has also been demonstrated to regulate localisation of signalling proteins such as P-Rex 1 (Pan et al., 2016), suggesting that it, in common with SMN, has a role in intra-cellular trafficking. These neural-specific and trafficking roles suggest that further analysis of the interaction between NCDN and the Sm proteins may help to better understand the molecular mechanisms of pathogenesis in SMA.

Reciprocal affinity-purification of GFP-tagged and endogenous NCDN and Sm proteins (Fig 3A, B) validated the interaction detected in the interactome analysis. Although originally identified as a protein interacting with SmN but not SmB, further investigation indicates that NCDN is, in fact, capable of interacting with both of these Sm proteins. Of much greater interest, however, is the interaction documented between NCDN and SMN, which appears more robust than that between NCDN and the Sm proteins (Fig 3). Furthermore, NCDN localises with SMN and the Sm proteins in mobile vesicles in the neurites of SH-SY5Y cells (Fig 4), rather than in the nucleus, suggesting that it shares cytoplasmic, rather than nuclear, roles with SMN. The truncated protein SMNΔ7, which can't fully substitute for FL-SMN despite retaining some functionality, is largely restricted to the nucleus (Renvoise et al., 2006; Sleigh et al., 2011). While it can't yet be ruled out that SMNΔ7 lacks the capability to substitute for FL-SMN in nuclear roles, this suggests that cytoplasmic roles of SMN are key to SMA pathology. NCDN was not co-purified with splicing snRNPs, under conditions that showed a clear enrichment of SMN, a key assembly factor for snRNPs, in the snRNP fraction. This suggests that the interaction between NCDN, SMN and the Sm proteins is not related to snRNP assembly.

Potential consequences of NCDN mis-localisation associated with SMN reduction

We have identified co-localisation of both SMN and NCDN with a sub-set of Rab5 vesicles. Since NCDN is also found in a sub-set of SMN-positive cytoplasmic structures, it is highly likely that these are Rab5 vesicles. It is possible that the protein-protein interactions between NCDN and SMN occur elsewhere in the cytoplasm as both proteins also show a diffuse cytosolic pool, but the decrease seen in cytoplasmic structures containing NCDN following SMN depletion suggest that cellular pathways requiring NCDN-containing vesicles may be compromised in SMA. Loss of NCDN-positive cytoplasmic structures was seen in cells with a moderate reduction in SMN levels, so NCDN may be of relevance for patients with milder forms of SMA.

At present, the precise roles of NCDN are not fully understood, although it has been implicated in dendrite morphogenesis, neural outgrowth, synaptic plasticity regulation, and moderation of signalling pathways in neural cells (Dateki et al., 2005; Francke et al., 2006; Matosin et al., 2015; Ohoka et al., 2001; Oku et al., 2013; Pan et al., 2016; Shinozaki et al., 1999; Shinozaki et al., 1997; Wang et al., 2013; Wang et al., 2009; Ward et al., 2009). NCDN has also previously been shown to localise to Rab5 vesicles within dendrites (Oku et al., 2013). These dendritic Rab5 vesicles have been found have an important role in dendrite morphogenesis and somatodendritic polarity (Guo et al., 2016; Satoh et al., 2008). As we have now demonstrated that SMN localises to a sub-set of Rab5 vesicles, likely in association with NCDN, SMN may also be implicated in cell polarity, with an insufficiency of SMN causing problems with both establishment and maintenance of polarity. These would be particularly vital in such elongated cells as motor neurons and may be mediated through trafficking of mRNAs or proteins. Further work will be required to investigate defects in cell polarity as a pathogenic mechanism in SMA and their possible link to NCDN.

NCDN as a potential novel therapeutic target in SMA.

SMN has now been linked to several functions other than its canonical role in snRNP assembly. While reduction in the cell's capacity for snRNP assembly caused by lowered SMN may cause splicing defects, the key transcripts preferentially affecting motor neurones are still to be identified. SMN has an established role in the trafficking of mature mRNAs destined for localised translation. The nature of the structures involved in this role is not completely clear, however, with different authors describing the structures as vesicular or granular. Reduction of SMN has also been linked with endosomal defects, suggestive of the importance of SMN for vesicular transport. Here we provide further evidence for the presence of SMN in, or associated with, vesicles and document interactions between the essential neural protein, NCDN and SMN. Together with the clear enrichment of NCDN in motor neurones in mouse spinal cord, this suggests that NCDN may be a down-stream target of SMN reduction in SMA and places it as a potential target for therapy development in SMA. Further work will be required to establish which roles of NCDN also involve SMN, and whether these are of relevance for the molecular pathology of SMA. The co-dependence of SMN and NCDN in cytoplasmic vesicles, however, suggests that depletion of SMN, as seen in the majority of SMA patients, may affect NCDN localisation and/or function.

Materials and Methods

Plasmid constructs

pEGFP-SMN, pEYFP-SmB and mCherry-SmB have been described previously (Clelland et al., 2009; Sleeman et al., 2001; Sleeman and Lamond, 1999). pEYFP-SmN and pmCherry-SmN were generated by PCR amplification and sub-cloning cDNA of human SmN from SH-SY5Y cells into pEYFP-C1 and pmCherry-C1 respectively, using SNRPNEcoRI forward primer: TAGAATTCCATGACTGTTGGCAAGAGTAGC, and SNRPNBamHI reverse primer: TAGGATCCCTGAGATGGATCAACAGTATG. pmCherry-SMN was generated by PCR amplification sub-cloning the sequence from the pEGFP-SMN plasmid into pmCherry-C1 using an SMNEcoRI Forward primer: GCGGAATTCTATGGCGATGAGC and SMNBamHI Reverse Primer:

GCAGGATCCTTAATTTAAGGAATGTGA. To generate pEGFP-NCDN, NCDN cDNA from SH-SY5Y cells was PCR amplified and sub-cloned into a pEGFP-N3 plasmid using NCDNEcoRI forward primer: GCGGAATTCATGGCCTCGGATTGCG and NCDNSalI reverse primer: GCTGCTGACGGGCTCTGACAGGC. All cDNAs were amplified using GoTaq G2 (Promega, Madison, WI, USA) and the PCR products restriction digested using EcoRI and either BamHI or SalI (Promega), before ligation with T4 DNA ligase (Thermo Scientific, Waltham, MA, USA). mRFP-Rab5 was a gift from Ari Helenius (Vonderheit and Helenius, 2005).

Cell lines and cell culture

SH-SY5Y cells were from ATCC. Cells were cultured in DMEM with 10% FBS at 37°C, 5% CO_2. Transfections were carried out using Effectene (Qiagen, Hilden, Germany) according to the manufacturer's instructions. Stable SH-SY5Y cell lines expressing mCherry–SmB and GFP–SMN have been described previously (Clelland et al., 2009; Prescott et al., 2014). SH-SY5Y cell lines stably expressing YFP-SmN, YFP-SmB, YFP, mCherry-SmN and NCDN-GFP were derived by clonal isolation following selection with 200 µg/ml G418 (Roche, Basel, Switzerland) following transfection.

Animals

Mouse tissues in this study were obtained from littermate, healthy control mice (*Smn*$^{+/-}$; *SMN2*$^{tg/0}$) from the 'Taiwanese' model of SMA.(Hsieh-Li et al., 2000) Mice were originally obtained from Jackson Laboratories and were maintained in animal care facilities at the University of Edinburgh under standard specic pathogen–free conditions on a congenic FVB background. All animal breeding was done in accordance with University of Edinburgh institutional guidelines and under the appropriate project and personal licenses granted by the UK Home Office.

Immunostaining, microscopy and image analysis

Cell fixing and immunostaining were both carried out as described previously (Sleeman et al., 2003). Immunostaining of spinal cord sections was carried out as described previously (Powis and Gillingwater, 2016). Live cell and fixed cell microscopy and image processing were carried out as described previously (Prescott et al., 2014). BODIPY-493 (Life Technologies, Paisley, UK) was added

to culture medium at 2 µg/ml overnight. Antibodies used for immunostaining were mouse monoclonal Y12 anti-Smith (SmB) (Abcam, Cambridge, MA, USA, ab3138, 1:20), rabbit polyclonal 204-10 (anti-Coilin) (a gift from A. I. Lamond (Bohmann et al., 1995), 1:500), mouse monoclonal anti-SMN (BD Transduction, San Jose, CA, USA, 610646, 1:50), goat anti-ChAT (Millipore, Burlington, MA, USA, AB144P) and rabbit polyclonal anti-NCDN (Proteintech, Manchester, UK, 13187-1-AP, 1:50). Overlays of images were made using Adobe Photoshop CS5 (Adobe, San Jose, CA, USA). Co-localisation images were generated using Volocity 6.3 (PerkinElmer, Waltham, MA, USA), using automatic thresholds on non-deconvolved images. Co-localisation values of 0.05 or less were excluded as this was the maximum co-localisation value observed between mCherry signal and YFP signal in neurites expressing YFP as a control together with mCherry-tagged proteins of interest. Deconvolution was also performed using Volocity 6.3, with between 15 and 25 iterations of deconvolution. Images of spinal cord sections collected using a 60x objective on a DeltaVision RT microscope (Applied Precision) were assembled into panels using the FIJI (Schindelin et al., 2012) plug-in and a custom written export protocol.

Statistical Analysis, and generation of graphs

Data was processed using Microsoft Excel (Microsoft) to produce ratios, proportions and percentages. Bar charts, Box and Whisker plots were then generated using Prism 6 (GraphPad, La Jolla, CA, USA) from the processed data. Statistical analysis was also performed using Prism 6, with multiple comparisons to determine statistical difference between specific sets of data. Tukey post-tests were used to identify outliers in Anova statistical analysis.

Preparation of cell lysates and immunoblotting

Cells were grown in 10cm diameter dishes, before being detached with trypsin and collected by centrifugation at 180 RCF for 5 minutes. The cell pellet was washed 3 times in PBS before lysis in 100µl of ice cold lysis buffer per dish (50 mM Tris-HCl pH 7.5; 0.5 M NaCl; 1% (v/v) Nonidet P-40; 1% (w/v) sodium deoxycholate; 0.1% (w/v) SDS; 2 mM EDTA plus cOmplete mini EDTA-free protease inhibitor cocktail (Roche, one tablet per 10 ml)), followed by homogenisation by sonication. Isolation of YFP/GFP and mCherry/mRFP- tagged proteins was carried out as described previously with GFP- or RFP-Trap (Chromotek, Planegg-Martinsried, Germany)(Prescott et al., 2014). Immuno-precipitation of endogenous SMN from brain lysate was carried out as described previously using mouse monoclonal anti-SMN (BD Transduction labs 610646) (Boyd et al., 2017; Groen et al., 2013). Lysates were electrophoresed on a 10% SDS-polyacrylamide gel and

transferred to nitro-cellulose (Hybond-C+ or Protran premium 0.2μm, both GE Healthcare, Little Chalfont, UK) membranes for immunoblotting. Antibodies used were rat monoclonal anti-RFP (Chromotek 5F8, 1 : 500); goat polyclonal anti-γCOP (Santa Cruz, Dallas, TX, USA, sc-14167, 1 : 250), rabbit polyclonal anti-GFP (Abcam ab290, 1:2000), rabbit polyclonal anti-SNRPN (SmN) (Proteintech 11070-1-AP, 1:800), mouse monoclonal Y12 anti-Smith (SmB) (Abcam ab3138, 1:100), rabbit polyclonal anti-SMN (Santa Cruz sc-15320, 1:500), mouse monoclonal anti-SMN (BD Transduction labs 610646, 1:500), rabbit polyclonal anti-COPB1 (CUSAB, College Park, MD, USA, CSB-PA005783LA01HU, 1:500), mouse monoclonal anti-Lamin A/C (Santa Cruz sc-7292, 1:500), rabbit polyclonal anti-NCDN (Proteintech 13187-1-AP, 1:500), mouse Monoclonal anti-tubulin (Sigma Aldrich, St Louis, MO, USA, 1:500) and rabbit polyclonal anti-Histone H3 (Proteintech 17168-1-AP, 1:300). Secondary antibodies were goat anti-rabbit Dylight 700 (Thermo Scientific 35569, 1:15,000) or goat anti-mouse Dylight 800 (Thermo Scientific SA5-10176, 1:15,000). Alternatively, goat anti-mouse IRDye 800CW (Li-Cor 925-32210, 1:25,000) and goat anti-rabbit IRDye 680RD (Li-Cor 925-68071, 1:25,000) were used. Goat anti-Rat Dylight 800 (Thermo Scientific, SA5-10024) antibody was used to visualise the rat monoclonal anti-RFP antibody at a concentration of 1:15,000. Donkey anti-goat IRDye 800CW (Licor, Lincoln, NE, USA, 925-32214) was used at a concentration of 1:25,000 to detect goat polyclonal anti-γCOP. Donkey anti-rabbit conjugated to horseradish peroxidase (HRP) (Pierce, Waltham, MA, USA, 31460, 1:15,000) was used to identify endogenous NCDN in figure 3D. Detection of antibodies conjugated to fluorophores was carried out with an Odessey CLx using Image Studio (both Li-cor). Band quantification was also performed using Image Studio. Detection of antibodies conjugated to peroxidase was performed using ECL Western Blotting Substrate (Pierce) and developed with Hyperfilm (Amersham), using a Kodak X-OMAT 1000 developer, after 30-45 minutes exposure.

Immunoprecipitation of intact snRNPs

To immunoprecipitate intact snRNPS, whole cell lysates were incubated with anti-2,2,7-trimethylguanosine conjugated to agarose beads (Millipore NA02A), with Sepharose 4B beads (Sigma Aldrich) as a control. 40 ng of pre-cleared lysate and unbound protein were separated by SDS-PAGE alongside material precipitated with Sepharose control beads and TMG antibody beads. Subsequent detection was carried out using rabbit anti-GFP (1:2000, Abcam), rat mAb anti-RFP (1:500, Chromotek), mouse monoclonal anti-SMN (1:500, BD Transduction labs) and rabbit polyclonal anti-SNRPN (1:800, Proteintech).

Preparations and analysis of Mass Spectrometry samples

SH-SY5Y cells constitutively expressing either YFP, YFP-SmN or YFP-SmB were lysed in co-immunoprecipitation buffer (10mM Tris pH7.5, 150mM NaCl, 0.5mM EDTA, 0.5% NP40, 1 cOmplete EDTA-free protease inhibitor tablet (Roche) per 10ml), followed by affinity purification of the tagged proteins with GFP-Trap as above. 11mg of total protein per sample was used as input. 5µl of the affinity isolated material, alongside precleared lysate and unbound lysate was transferred to nitrocellulose membrane (as above) and immunodetected using Rabbit anti-GFP (Abcam) to confirm efficient immunoprecipitation. Samples were then electrophoresed on a NuPAGE 4-12% Bis-Tris Acrylamide gel (Novex, Waltham, MA, USA, NP0321), Coomassie stained using SimplyBlue SafeStain (Invitrogen, Paisley, UK), gel chunks excised and analysed by the Mass Spectrometry and Proteomics Facility at the University of St Andrews.

The gel chunks were cut into 1 mm cubes. These were then subjected to in-gel digestion, using a ProGest Investigator in-gel digestion robot (Digilab, Hopkinton, MA, USA) using standard protocols (Shevchenko et al., 1996). Briefly, the gel cubes were destained by washing with MeCN and subjected to reduction with DTT and alkylation with IAA before digestion overnight with trypsin at 37°C. The peptides were extracted with 10% formic acid, and the volume reduced to ~20ul by concentration in a speedvac (Thermo Scientific).

The peptides were then injected onto an Acclaim PepMap 100 C18 trap and an Acclaim PepMap RSLC C18 column (ThermoFisher Scientific), using a nanoLC Ultra 2D plus loading pump and nanoLC as-2 autosampler (Eksigent). The peptides were eluted with a gradient of increasing acetonitrile, containing 0.1 % formic acid (2-20% acetonitrile in 90 min, 20-40% in a further 30 min, followed by 98% acetonitrile to clean the column, before re-equilibration to 2% acetonitrile). The eluate was sprayed directly into a TripleTOF 5600 electrospray tandem mass spectrometer (Sciex, Foster City, CA) and analysed in Information Dependent Acquisition (IDA) mode, performing 250 msec of MS followed by 100 msec MS/MS analyses on the 20 most intense peaks seen by MS. The MS/MS data files generated were analysed using the ProteinPilot Paragon search algorithm v5.0.1 (Sciex) against the NCBInr database (Nov 2012) restricting the search to Homo sapiens, with trypsin as the digestion enzyme and selecting cysteine alkylation with iodoacetamide, 'Gel based ID' as a 'Special factor', 'Biological modifications' as the 'ID Focus' and a 'Thorough' 'Search effort'.

ProteinPilot also performs a decoy database search to assess the False Discovery Rate. Protein identifications were accepted if they were identified by at least 2 peptides with the Detected Protein Threshold set at 0.05. The data was also analysed via the 'Create mgf file' script in PeakView (Sciex) using the Mascot search algorithm (Matrix Science), against the NCBInr database (Oct 2014) restricting the search to Homo sapiens (284,317 sequences), trypsin as the cleavage enzyme and carbamidomethyl as a fixed modification of cysteines and methionine oxidation as a variable modification. The peptide mass tolerance was set to ± 0.05 Da and the MSMS mass tolerance to ± 0.1 Da. Scaffold viewer (version Scaffold_4.5.1, Proteome Software) was used to validate the identifications from Mascot. Peptide identifications were accepted if they could be established at greater than 95.0% probability by the Peptide Prophet algorithm (Keller et al., 2002). Protein identifications were accepted if they could be established at greater than 99.0% probability and contained at least 2 identified peptides. Protein probabilities were assigned by the Protein Prophet algorithm (Nesvizhskii et al., 2003). Proteins that contained similar peptides and could not be differentiated based on MS/MS analysis alone were grouped to satisfy the principles of parsimony.

Identified proteins affinity purified alongside YFP-SmB or YFP-SmN were discounted if they were additionally identified as being affinity purified with YFP, or if they were present within the Sepharose bead proteome (Trinkle-Mulcahy et al., 2008). The mass spectrometry proteomics data have been deposited to the ProteomeXchange Consortium via the PRIDE (Vizcaino et al., 2016) partner repository with the dataset identifier PXD008710.

RNAi assays

Reduction of protein expression using siRNA was achieved by transfecting the appropriate cell lines with siRNAs (Dharmacon, Lafayette, CO, USA) using Viromer Green (Lipocalyx GmbH, Halle (Saale), Germany) according to the manufacturer's instructions. Cells were lysed for assay by immunoblotting, or fixed with paraformaldehyde for fluorescence microscopy, 48 hours after transfection. Sequences used were SMN: CAGUGGAAAGUUGGGGACA; SmB, a mixture of CCCACAAGGAAGAGGUACU, GCAUAUUGAUUACAGGAUG, CCGUAAGGCUGUACAUAGU, CAAUGACAGUAGAGGGACC; NCDN, individually and a mixture of NCDN 18 GUUCAUUGGUGACGAGAAA, NCDN 19 AGACCUCAUCCUUGCGUAA, NCDN 20 AGGCCAAGAAUGACAGCGA, NCDN 21 GGCCAUUGAUAUCGCAGUU; negative control (siControl) targeting luciferase, UAAGGCUAUGAAGAGAUAC; positive control targeting Lamin A/C,

GGUGGUGACGAUCUGGGCU; SiGlo Cyclophillin B to determine transfection efficiency, GGAAAGACUGUUCCAAAAA. Lysates were electrophoresed on an SDS-PAGE gel, transferred to nitrocellulose membrane, and immunodetected with antibodies to the above proteins. Band signal intensity determined with ImageStudio (Li-Cor), and the values were normalised to tubulin, following correction for background. Reduction of protein expression using shRNA was achieved by transfecting SH-SH5Y cell lines with pSUPER-GFP.Neo plasmids (Oligoengine, Seattle, WA, USA) expressing shRNA to SMN and Cyclophilin B, which have been described previously (Clelland et al., 2012) using Effectene (QIAGEN).

Fractionation

Cells were pelleted from the appropriate cell line, and incubated in Buffer A (10mM HEPES pH7.9, 1.5mM $MgCl_2$, 10mM KCl, 0.5mM DTT, 1 cOmplete EDTA-free protease inhibitor tablet per 10ml) for 5 minutes, before being Dounce homogenised 25 times using the tight pestle to disrupt the plasma membrane. This was then centrifuged at 300 RCF for 5 minutes to pellet the nuclei. The supernatant was removed, recentrifuged at 300 RCF to further remove nuclei, before the supernatant was centrifuged at 16,100 RCF for 30 minutes using a refrigerated 5415R Centrifuge (Eppendorf, Hamburg, Germany). The nuclei were resuspended in Buffer S1 (250mM Sucrose, 10mM $MgCl_2$), before this was layered over with Buffer S3 (880mM Sucrose, 0.5mM $MgCl_2$). The nuclear pellet was then centrifuged at 2800 RCF for 10 minutes to wash and pellet the nuclei. The supernatant from the 16,100 RCF centrifugation was further centrifuged at 100,000 RCF using an Optima Max-XP ultracentrifuge with a TLA-110 Rotor (Beckman-Coulter, Brea, CA, USA) for 60 minutes. The supernatant was removed and kept. The 16,100 and 100,000 RCF pellets were washed in Buffer A and centrifuged at 16,100 RCF for 30 minutes or 100,000 RCF for 1 hour respectively. Each pellet was then resuspended in lysis buffer (see above). To confirm efficient separation of cytoplasmic fractions from the nuclear fractions, Mouse anti-tubulin (Sigma Aldrich, 1:500) and Rabbit polyclonal anti-Histone H3 (Proteintech, 1:300) antibodies were used.

Acknowledgements

The authors thank Prof. Ari Helenius (ETH Zurich) for the mRFP-Rab5 construct, Prof Gary Bassell, Emory University for the pGFP-SMNΔ7 construct and Prof. Angus Lamond (University of Dundee) for anti-coilin antibodies. Assistance using FIGI for construction of panelled images of spinal cord sections was provided by Alan Prescott and Graeme Ball (University of Dundee).

Competing Interests

The use of NCDN as a modulator compound for developing SMA therapies is the subject of patent application GB1710433.2 filed 29 June 2017 at the UK IPO.

Funding Statement

Work in the Sleeman laboratory by Luke Thompson was funded by the Medical Research Council, UK [MRC-CASE studentship MR/K016997/1]. This work was also supported by Wellcome Trust [grant number 094476/Z/10/Z], which funded the purchase of the TripleTOF 5600 mass spectrometer at the BSRC Mass Spectrometry and Proteomics Facility, University of St Andrews and Wellcome Trust ISSF funding [105621/Z/14/Z], Wellcome Trust 106098/Z/14/Z (to E.J.N.G and T.H.G) and the UK SMA Research Consortium (SMA Trust, to T.H.G.).

Data Availability

The mass spectrometry proteomics data have been deposited to the ProteomeXchange Consortium via the PRIDE (Vizcaino et al., 2016) partner repository with the dataset identifier PXD008710.

Author contributions:

LWT designed experiments, generated reagents, produced and analysed data, generated the figures and helped to prepare and edit the manuscript. KM acquired and analysed data. EG and TG designed experiments and produced data. SS and CB processed the MS samples, produced the MS/MS data set and assisted with analysis. JES came up with the original concept, designed experiments, analysed data and prepared and edited the manuscript.

References

Akten, B., Kye, M. J., Hao le, T., Wertz, M. H., Singh, S., Nie, D., Huang, J., Merianda, T. T., Twiss, J. L., Beattie, C. E. et al. (2011). Interaction of survival of motor neuron (SMN) and HuD proteins with mRNA cpg15 rescues motor neuron axonal deficits. *Proc Natl Acad Sci U S A* **108**, 10337-42.

Azzouz, T. N., Pillai, R. S., Dapp, C., Chari, A., Meister, G., Kambach, C., Fischer, U. and Schumperli, D. (2005). Toward an assembly line for U7 snRNPs: interactions of U7-specific Lsm proteins with PRMT5 and SMN complexes. *J Biol Chem* **280**, 34435-40.

Battle, D. J., Kasim, M., Yong, J., Lotti, F., Lau, C. K., Mouaikel, J., Zhang, Z., Han, K., Wan, L. and Dreyfuss, G. (2006). The SMN complex: an assembly machine for RNPs. *Cold Spring Harb Symp Quant Biol* **71**, 313-20.

Benecke, H., Luhrmann, R. and Will, C. L. (2005). The U11/U12 snRNP 65K protein acts as a molecular bridge, binding the U12 snRNA and U11-59K protein. *EMBO J* **24**, 3057-69.

Bohmann, K., Ferreira, J. A. and Lamond, A. I. (1995). Mutational analysis of p80 coilin indicates a functional interaction between coiled bodies and the nucleolus. *J Cell Biol* **131**, 817-31.

Boulisfane, N., Choleza, M., Rage, F., Neel, H., Soret, J. and Bordonne, R. (2011). Impaired minor tri-snRNP assembly generates differential splicing defects of U12-type introns in lymphoblasts derived from a type I SMA patient. *Hum Mol Genet* **20**, 641-8.

Bowerman, M., Shafey, D. and Kothary, R. (2007). Smn depletion alters profilin II expression and leads to upregulation of the RhoA/ROCK pathway and defects in neuronal integrity. *J Mol Neurosci* **32**, 120-31.

Boyd, P. J., Tu, W. Y., Shorrock, H. K., Groen, E. J. N., Carter, R. N., Powis, R. A., Thomson, S. R., Thomson, D., Graham, L. C., Motyl, A. A. L. et al. (2017). Bioenergetic status modulates motor neuron vulnerability and pathogenesis in a zebrafish model of spinal muscular atrophy. *PLoS Genet* **13**, e1006744.

Bucci, C., Parton, R. G., Mather, I. H., Stunnenberg, H., Simons, K., Hoflack, B. and Zerial, M. (1992). The small GTPase rab5 functions as a regulatory factor in the early endocytic pathway. *Cell* **70**, 715-28.

Campbell, L., Potter, A., Ignatius, J., Dubowitz, V. and Davies, K. (1997). Genomic variation and gene conversion in spinal muscular atrophy: implications for disease process and clinical phenotype. *Am J Hum Genet* **61**, 40-50.

Chen, Y., Xu, Y., Li, G., Li, N., Yu, T., Yao, R. E., Wang, X., Shen, Y. and Wang, J. (2017). Exome Sequencing Identifies De Novo DYNC1H1 Mutations Associated With Distal Spinal Muscular Atrophy and Malformations of Cortical Development. *J Child Neurol* **32**, 379-386.

Clelland, A. K., Bales, A. B. and Sleeman, J. E. (2012). Changes in intranuclear mobility of mature snRNPs provide a mechanism for splicing defects in spinal muscular atrophy. *J Cell Sci* **125**, 2626-37.

Clelland, A. K., Kinnear, N. P., Oram, L., Burza, J. and Sleeman, J. E. (2009). The SMN protein is a key regulator of nuclear architecture in differentiating neuroblastoma cells. *Traffic* **10**, 1585-98.

Corey, D. R. (2017). Nusinersen, an antisense oligonucleotide drug for spinal muscular atrophy. *Nat Neurosci* **20**, 497-499.

Custer, S. K., Gilson, T. D., Li, H., Todd, A. G., Astroski, J. W., Lin, H., Liu, Y. and Androphy, E. J. (2016). Altered mRNA Splicing in SMN-Depleted Motor Neuron-Like Cells. *PLoS One* **11**, e0163954.

Custer, S. K., Todd, A. G., Singh, N. N. and Androphy, E. J. (2013). Dilysine motifs in exon 2b of SMN protein mediate binding to the COPI vesicle protein alpha-COP and neurite outgrowth in a cell culture model of spinal muscular atrophy. *Hum Mol Genet* **22**, 4043-52.

Dateki, M., Horii, T., Kasuya, Y., Mochizuki, R., Nagao, Y., Ishida, J., Sugiyama, F., Tanimoto, K., Yagami, K., Imai, H. et al. (2005). Neurochondrin negatively regulates CaMKII phosphorylation, and nervous system-specific gene disruption results in epileptic seizure. *J Biol Chem* **280**, 20503-8.

De Duve, C. (1971). Tissue fractionation. Past and present. *J Cell Biol* **50**, 20d-55d.

Dimitriadi, M., Derdowski, A., Kalloo, G., Maginnis, M. S., O'Hern, P., Bliska, B., Sorkac, A., Nguyen, K. C., Cook, S. J., Poulogiannis, G. et al. (2016). Decreased function of survival motor neuron protein impairs endocytic pathways. *Proc Natl Acad Sci U S A* **113**, E4377-86.

Ding, D., Chen, Z., Li, K., Long, Z., Ye, W., Tang, Z., Xia, K., Qiu, R., Tang, B. and Jiang, H. (2016). Identification of a de novo DYNC1H1 mutation via WES according to published guidelines. *Sci Rep* **6**, 20423.

Doktor, T. K., Hua, Y., Andersen, H. S., Broner, S., Liu, Y. H., Wieckowska, A., Dembic, M., Bruun, G. H., Krainer, A. R. and Andresen, B. S. (2017). RNA-sequencing of a mouse-model of spinal muscular atrophy reveals tissue-wide changes in splicing of U12-dependent introns. *Nucleic Acids Res* **45**, 395-416.

Doyle, M. and Kiebler, M. A. (2011). Mechanisms of dendritic mRNA transport and its role in synaptic tagging. *EMBO J* **30**, 3540-52.

Fallini, C., Donlin-Asp, P. G., Rouanet, J. P., Bassell, G. J. and Rossoll, W. (2016). Deficiency of the Survival of Motor Neuron Protein Impairs mRNA Localization and Local Translation in the Growth Cone of Motor Neurons. *J Neurosci* **36**, 3811-20.

Fallini, C., Rouanet, J. P., Donlin-Asp, P. G., Guo, P., Zhang, H., Singer, R. H., Rossoll, W. and Bassell, G. J. (2014). Dynamics of survival of motor neuron (SMN) protein interaction with the mRNA-binding protein IMP1 facilitates its trafficking into motor neuron axons. *Dev Neurobiol* **74**, 319-332.

Fallini, C., Zhang, H., Su, Y., Silani, V., Singer, R. H., Rossoll, W. and Bassell, G. J. (2011). The survival of motor neuron (SMN) protein interacts with the mRNA-binding protein HuD and regulates localization of poly(A) mRNA in primary motor neuron axons. *J Neurosci* **31**, 3914-25.

Finkel, R. S., Chiriboga, C. A., Vajsar, J., Day, J. W., Montes, J., De Vivo, D. C., Yamashita, M., Rigo, F., Hung, G., Schneider, E. et al. (2016). Treatment of infantile-onset spinal muscular atrophy with nusinersen: a phase 2, open-label, dose-escalation study. *Lancet* **388**, 3017-3026.

Fischer, U., Englbrecht, C. and Chari, A. (2011). Biogenesis of spliceosomal small nuclear ribonucleoproteins. *Wiley Interdiscip Rev RNA* **2**, 718-31.

Fischer, U., Liu, Q. and Dreyfuss, G. (1997). The SMN-SIP1 complex has an essential role in spliceosomal snRNP biogenesis. *Cell* **90**, 1023-9.

Francke, F., Ward, R. J., Jenkins, L., Kellett, E., Richter, D., Milligan, G. and Bachner, D. (2006). Interaction of neurochondrin with the melanin-concentrating hormone receptor 1 interferes with G protein-coupled signal transduction but not agonist-mediated internalization. *J Biol Chem* **281**, 32496-507.

Gabanella, F., Butchbach, M. E., Saieva, L., Carissimi, C., Burghes, A. H. and Pellizzoni, L. (2007). Ribonucleoprotein assembly defects correlate with spinal muscular atrophy severity and preferentially affect a subset of spliceosomal snRNPs. *PLoS One* **2**, e921.

Giesemann, T., Rathke-Hartlieb, S., Rothkegel, M., Bartsch, J. W., Buchmeier, S., Jockusch, B. M. and Jockusch, H. (1999). A role for polyproline motifs in the spinal muscular atrophy protein SMN. Profilins bind to and colocalize with smn in nuclear gems. *J Biol Chem* **274**, 37908-14.

Gonsalvez, G. B., Rajendra, T. K., Wen, Y., Praveen, K. and Matera, A. G. (2010). Sm proteins specify germ cell fate by facilitating oskar mRNA localization. *Development* **137**, 2341-51.

Groen, E. J., Fumoto, K., Blokhuis, A. M., Engelen-Lee, J., Zhou, Y., van den Heuvel, D. M., Koppers, M., van Diggelen, F., van Heest, J., Demmers, J. A. et al. (2013). ALS-associated mutations in FUS disrupt the axonal distribution and function of SMN. *Hum Mol Genet* **22**, 3690-704.

Guo, X., Farias, G. G., Mattera, R. and Bonifacino, J. S. (2016). Rab5 and its effector FHF contribute to neuronal polarity through dynein-dependent retrieval of somatodendritic proteins from the axon. *Proc Natl Acad Sci U S A* **113**, E5318-27.

Hao le, T., Wolman, M., Granato, M. and Beattie, C. E. (2012). Survival motor neuron affects plastin 3 protein levels leading to motor defects. *J Neurosci* **32**, 5074-84.

Harms, M. B., Allred, P., Gardner, R., Jr., Fernandes Filho, J. A., Florence, J., Pestronk, A., Al-Lozi, M. and Baloh, R. H. (2010). Dominant spinal muscular atrophy with lower extremity predominance: linkage to 14q32. *Neurology* **75**, 539-46.

Harms, M. B., Ori-McKenney, K. M., Scoto, M., Tuck, E. P., Bell, S., Ma, D., Masi, S., Allred, P., Al-Lozi, M., Reilly, M. M. et al. (2012). Mutations in the tail domain of DYNC1H1 cause dominant spinal muscular atrophy. *Neurology* **78**, 1714-20.

Hausmann, S., Zheng, S., Costanzo, M., Brost, R. L., Garcin, D., Boone, C., Shuman, S. and Schwer, B. (2008). Genetic and biochemical analysis of yeast and human cap trimethylguanosine synthase: functional overlap of 2,2,7-trimethylguanosine caps, small nuclear ribonucleoprotein components, pre-mRNA splicing factors, and RNA decay pathways. *J Biol Chem* **283**, 31706-18.

Heesen, L., Peitz, M., Torres-Benito, L., Holker, I., Hupperich, K., Dobrindt, K., Jungverdorben, J., Ritzenhofen, S., Weykopf, B., Eckert, D. et al. (2016). Plastin 3 is upregulated in iPSC-derived motoneurons from asymptomatic SMN1-deleted individuals. *Cell Mol Life Sci* **73**, 2089-104.

Holt, C. E. and Schuman, E. M. (2013). The central dogma decentralized: new perspectives on RNA function and local translation in neurons. *Neuron* **80**, 648-57.

Hosseinibarkooie, S., Peters, M., Torres-Benito, L., Rastetter, R. H., Hupperich, K., Hoffmann, A., Mendoza-Ferreira, N., Kaczmarek, A., Janzen, E., Milbradt, J. et al. (2016). The Power of Human Protective Modifiers: PLS3 and CORO1C Unravel Impaired Endocytosis in Spinal Muscular Atrophy and Rescue SMA Phenotype. *Am J Hum Genet* **99**, 647-665.

Hosseinibarkooie, S., Schneider, S. and Wirth, B. (2017). Advances in understanding the role of disease-associated proteins in spinal muscular atrophy. *Expert Rev Proteomics* **14**, 581-592.

Hsieh-Li, H. M., Chang, J. G., Jong, Y. J., Wu, M. H., Wang, N. M., Tsai, C. H. and Li, H. (2000). A mouse model for spinal muscular atrophy. *Nat Genet* **24**, 66-70.

Hua, Y. and Zhou, J. (2004). Survival motor neuron protein facilitates assembly of stress granules. *FEBS Lett* **572**, 69-74.

Huber, K. M., Kayser, M. S. and Bear, M. F. (2000). Role for rapid dendritic protein synthesis in hippocampal mGluR-dependent long-term depression. *Science* **288**, 1254-7.

Huntriss, J. D., Latchman, D. S. and Williams, D. G. (1993). The snRNP core protein SmB and tissue-specific SmN protein are differentially distributed between snRNP particles. *Nucleic Acids Res* **21**, 4047-53.

Huo, Q., Kayikci, M., Odermatt, P., Meyer, K., Michels, O., Saxena, S., Ule, J. and Schumperli, D. (2014). Splicing changes in SMA mouse motoneurons and SMN-depleted neuroblastoma cells: evidence for involvement of splicing regulatory proteins. *RNA Biol* **11**, 1430-46.

Jablonka, S., Schrank, B., Kralewski, M., Rossoll, W. and Sendtner, M. (2000). Reduced survival motor neuron (Smn) gene dose in mice leads to motor neuron degeneration: an animal model for spinal muscular atrophy type III. *Hum Mol Genet* **9**, 341-6.

Jeronimo, C., Forget, D., Bouchard, A., Li, Q., Chua, G., Poitras, C., Therien, C., Bergeron, D., Bourassa, S., Greenblatt, J. et al. (2007). Systematic analysis of the protein interaction network for the human transcription machinery reveals the identity of the 7SK capping enzyme. *Mol Cell* **27**, 262-74.

Kang, H. and Schuman, E. M. (1996). A requirement for local protein synthesis in neurotrophin-induced hippocampal synaptic plasticity. *Science* **273**, 1402-6.

Keller, A., Nesvizhskii, A. I., Kolker, E. and Aebersold, R. (2002). Empirical statistical model to estimate the accuracy of peptide identifications made by MS/MS and database search. *Anal Chem* **74**, 5383-92.

Le, T. T., Pham, L. T., Butchbach, M. E., Zhang, H. L., Monani, U. R., Coovert, D. D., Gavrilina, T. O., Xing, L., Bassell, G. J. and Burghes, A. H. (2005). SMNDelta7, the major product of the centromeric survival motor neuron (SMN2) gene, extends survival in mice with spinal muscular atrophy and associates with full-length SMN. *Hum Mol Genet* **14**, 845-57.

Lee, M. S., Lin, Y. S., Deng, Y. F., Hsu, W. T., Shen, C. C., Cheng, Y. H., Huang, Y. T. and Li, C. (2014). Modulation of alternative splicing by expression of small nuclear ribonucleoprotein polypeptide N. *FEBS J* **281**, 5194-207.

Lefebvre, S., Burglen, L., Reboullet, S., Clermont, O., Burlet, P., Viollet, L., Benichou, B., Cruaud, C., Millasseau, P., Zeviani, M. et al. (1995). Identification and characterization of a spinal muscular atrophy-determining gene. *Cell* **80**, 155-65.

Lefebvre, S., Burlet, P., Liu, Q., Bertrandy, S., Clermont, O., Munnich, A., Dreyfuss, G. and Melki, J. (1997). Correlation between severity and SMN protein level in spinal muscular atrophy. *Nat Genet* **16**, 265-9.

Li, D. K., Tisdale, S., Lotti, F. and Pellizzoni, L. (2014). SMN control of RNP assembly: from post-transcriptional gene regulation to motor neuron disease. *Semin Cell Dev Biol* **32**, 22-9.

Li, H., Custer, S. K., Gilson, T., Hao le, T., Beattie, C. E. and Androphy, E. J. (2015). alpha-COP binding to the survival motor neuron protein SMN is required for neuronal process outgrowth. *Hum Mol Genet* **24**, 7295-307.

Liu, Q. and Dreyfuss, G. (1996). A novel nuclear structure containing the survival of motor neurons protein. *EMBO J* **15**, 3555-65.

Liu, Q., Fischer, U., Wang, F. and Dreyfuss, G. (1997). The spinal muscular atrophy disease gene product, SMN, and its associated protein SIP1 are in a complex with spliceosomal snRNP proteins. *Cell* **90**, 1013-21.

Lorson, C. L. and Androphy, E. J. (2000). An exonic enhancer is required for inclusion of an essential exon in the SMA-determining gene SMN. *Hum Mol Genet* **9**, 259-65.

Lorson, C. L., Hahnen, E., Androphy, E. J. and Wirth, B. (1999). A single nucleotide in the SMN gene regulates splicing and is responsible for spinal muscular atrophy. *Proc Natl Acad Sci U S A* **96**, 6307-11.

Lotti, F., Imlach, W. L., Saieva, L., Beck, E. S., Hao le, T., Li, D. K., Jiao, W., Mentis, G. Z., Beattie, C. E., McCabe, B. D. et al. (2012). An SMN-dependent U12 splicing event essential for motor circuit function. *Cell* **151**, 440-54.

Martinez-Carrera, L. A. and Wirth, B. (2015). Dominant spinal muscular atrophy is caused by mutations in BICD2, an important golgin protein. *Front Neurosci* **9**, 401.

Matosin, N., Fernandez-Enright, F., Fung, S. J., Lum, J. S., Engel, M., Andrews, J. L., Huang, X. F., Weickert, C. S. and Newell, K. A. (2015). Alterations of mGluR5 and its endogenous regulators Norbin, Tamalin and Preso1 in schizophrenia: towards a model of mGluR5 dysregulation. *Acta Neuropathol* **130**, 119-29.

Meister, G., Buhler, D., Pillai, R., Lottspeich, F. and Fischer, U. (2001). A multiprotein complex mediates the ATP-dependent assembly of spliceosomal U snRNPs. *Nat Cell Biol* **3**, 945-9.

Meister, G. and Fischer, U. (2002). Assisted RNP assembly: SMN and PRMT5 complexes cooperate in the formation of spliceosomal UsnRNPs. *EMBO J* **21**, 5853-63.

Monani, U. R. (2005). Spinal muscular atrophy: a deficiency in a ubiquitous protein; a motor neuron-specific disease. *Neuron* **48**, 885-96.

Monani, U. R., Lorson, C. L., Parsons, D. W., Prior, T. W., Androphy, E. J., Burghes, A. H. and McPherson, J. D. (1999). A single nucleotide difference that alters splicing patterns distinguishes the SMA gene SMN1 from the copy gene SMN2. *Hum Mol Genet* **8**, 1177-83.

Monani, U. R., Sendtner, M., Coovert, D. D., Parsons, D. W., Andreassi, C., Le, T. T., Jablonka, S., Schrank, B., Rossoll, W., Prior, T. W. et al. (2000). The human centromeric survival motor neuron gene (SMN2) rescues embryonic lethality in Smn(-/-) mice and results in a mouse with spinal muscular atrophy. *Hum Mol Genet* **9**, 333-9.

Mourao, A., Bonnal, S., Soni, K., Warner, L., Bordonne, R., Valcarcel, J. and Sattler, M. (2016). Structural basis for the recognition of spliceosomal SmN/B/B' proteins by the RBM5 OCRE domain in splicing regulation. *Elife* **5**.

Nesvizhskii, A. I., Keller, A., Kolker, E. and Aebersold, R. (2003). A statistical model for identifying proteins by tandem mass spectrometry. *Anal Chem* **75**, 4646-58.

Neveling, K., Martinez-Carrera, L. A., Holker, I., Heister, A., Verrips, A., Hosseini-Barkooie, S. M., Gilissen, C., Vermeer, S., Pennings, M., Meijer, R. et al. (2013). Mutations in BICD2, which encodes a golgin and important motor adaptor, cause congenital autosomal-dominant spinal muscular atrophy. *Am J Hum Genet* **92**, 946-54.

Niu, Q., Wang, X., Shi, M. and Jin, Q. (2015). A novel DYNC1H1 mutation causing spinal muscular atrophy with lower extremity predominance. *Neurol Genet* **1**, e20.

Nolle, A., Zeug, A., van Bergeijk, J., Tonges, L., Gerhard, R., Brinkmann, H., Al Rayes, S., Hensel, N., Schill, Y., Apkhazava, D. et al. (2011). The spinal muscular atrophy disease protein SMN is linked to the Rho-kinase pathway via profilin. *Hum Mol Genet* **20**, 4865-78.

Oates, E. C., Rossor, A. M., Hafezparast, M., Gonzalez, M., Speziani, F., MacArthur, D. G., Lek, M., Cottenie, E., Scoto, M., Foley, A. R. et al. (2013). Mutations in BICD2 cause dominant congenital spinal muscular atrophy and hereditary spastic paraplegia. *Am J Hum Genet* **92**, 965-73.

Ohoka, Y., Hirotani, M., Sugimoto, H., Fujioka, S., Furuyama, T. and Inagaki, S. (2001). Semaphorin 4C, a transmembrane semaphorin, [corrected] associates with a neurite-outgrowth-related protein, SFAP75. *Biochem Biophys Res Commun* **280**, 237-43.

Oku, S., Takahashi, N., Fukata, Y. and Fukata, M. (2013). In silico screening for palmitoyl substrates reveals a role for DHHC1/3/10 (zDHHC1/3/11)-mediated neurochondrin palmitoylation in its targeting to Rab5-positive endosomes. *J Biol Chem* **288**, 19816-29.

Oprea, G. E., Krober, S., McWhorter, M. L., Rossoll, W., Muller, S., Krawczak, M., Bassell, G. J., Beattie, C. E. and Wirth, B. (2008). Plastin 3 is a protective modifier of autosomal recessive spinal muscular atrophy. *Science* **320**, 524-7.

Ozcelik, T., Leff, S., Robinson, W., Donlon, T., Lalande, M., Sanjines, E., Schinzel, A. and Francke, U. (1992). Small nuclear ribonucleoprotein polypeptide N (SNRPN), an expressed gene in the Prader-Willi syndrome critical region. *Nat Genet* **2**, 265-9.

Pan, D., Barber, M. A., Hornigold, K., Baker, M. J., Toth, J. M., Oxley, D. and Welch, H. C. (2016). Norbin Stimulates the Catalytic Activity and Plasma Membrane Localization of the Guanine-Nucleotide Exchange Factor P-Rex1. *J Biol Chem* **291**, 6359-75.

Passini, M. A., Bu, J., Richards, A. M., Kinnecom, C., Sardi, S. P., Stanek, L. M., Hua, Y., Rigo, F., Matson, J., Hung, G. et al. (2011). Antisense oligonucleotides delivered to the mouse CNS ameliorate symptoms of severe spinal muscular atrophy. *Sci Transl Med* **3**, 72ra18.

Peeters, K., Bervoets, S., Chamova, T., Litvinenko, I., De Vriendt, E., Bichev, S., Kancheva, D., Mitev, V., Kennerson, M., Timmerman, V. et al. (2015). Novel mutations in the DYNC1H1 tail domain refine the genetic and clinical spectrum of dyneinopathies. *Hum Mutat* **36**, 287-91.

Peeters, K., Litvinenko, I., Asselbergh, B., Almeida-Souza, L., Chamova, T., Geuens, T., Ydens, E., Zimon, M., Irobi, J., De Vriendt, E. et al. (2013). Molecular defects in the motor adaptor BICD2 cause proximal spinal muscular atrophy with autosomal-dominant inheritance. *Am J Hum Genet* **92**, 955-64.

Pellizzoni, L., Charroux, B., Rappsilber, J., Mann, M. and Dreyfuss, G. (2001). A functional interaction between the survival motor neuron complex and RNA polymerase II. *J Cell Biol* **152**, 75-85.

Pellizzoni, L., Yong, J. and Dreyfuss, G. (2002). Essential role for the SMN complex in the specificity of snRNP assembly. *Science* **298**, 1775-9.

Peter, C. J., Evans, M., Thayanithy, V., Taniguchi-Ishigaki, N., Bach, I., Kolpak, A., Bassell, G. J., Rossoll, W., Lorson, C. L., Bao, Z. Z. et al. (2011). The COPI vesicle complex binds and moves with survival motor neuron within axons. *Hum Mol Genet* **20**, 1701-11.

Piazzon, N., Schlotter, F., Lefebvre, S., Dodre, M., Mereau, A., Soret, J., Besse, A., Barkats, M., Bordonne, R., Branlant, C. et al. (2013). Implication of the SMN complex in the biogenesis and steady state level of the signal recognition particle. *Nucleic Acids Res* **41**, 1255-72.

Powis, R. A. and Gillingwater, T. H. (2016). Selective loss of alpha motor neurons with sparing of gamma motor neurons and spinal cord cholinergic neurons in a mouse model of spinal muscular atrophy. *J Anat* **228**, 443-51.

Prescott, A. R., Bales, A., James, J., Trinkle-Mulcahy, L. and Sleeman, J. E. (2014). Time-resolved quantitative proteomics implicates the core snRNP protein SmB together with SMN in neural trafficking. *J Cell Sci* **127**, 812-27.

Prior, T. W., Swoboda, K. J., Scott, H. D. and Hejmanowski, A. Q. (2004). Homozygous SMN1 deletions in unaffected family members and modification of the phenotype by SMN2. *Am J Med Genet A* **130A**, 307-10.

Punetha, J., Monges, S., Franchi, M. E., Hoffman, E. P., Cirak, S. and Tesi-Rocha, C. (2015). Exome Sequencing Identifies DYNC1H1 Variant Associated With Vertebral Abnormality and Spinal Muscular Atrophy With Lower Extremity Predominance. *Pediatr Neurol* **52**, 239-44.

Renvoise, B., Khoobarry, K., Gendron, M. C., Cibert, C., Viollet, L. and Lefebvre, S. (2006). Distinct domains of the spinal muscular atrophy protein SMN are required for targeting to Cajal bodies in mammalian cells. *J Cell Sci* **119**, 680-92.

Riessland, M., Kaczmarek, A., Schneider, S., Swoboda, K. J., Lohr, H., Bradler, C., Grysko, V., Dimitriadi, M., Hosseinibarkooie, S., Torres-Benito, L. et al. (2017). Neurocalcin Delta Suppression Protects against Spinal Muscular Atrophy in Humans and across Species by Restoring Impaired Endocytosis. *Am J Hum Genet* **100**, 297-315.

Rossoll, W., Jablonka, S., Andreassi, C., Kroning, A. K., Karle, K., Monani, U. R. and Sendtner, M. (2003). Smn, the spinal muscular atrophy-determining gene product, modulates axon growth and localization of beta-actin mRNA in growth cones of motoneurons. *J Cell Biol* **163**, 801-12.

Rossoll, W., Kroning, A. K., Ohndorf, U. M., Steegborn, C., Jablonka, S. and Sendtner, M. (2002). Specific interaction of Smn, the spinal muscular atrophy determining gene product, with hnRNP-R and gry-rbp/hnRNP-Q: a role for Smn in RNA processing in motor axons? *Hum Mol Genet* **11**, 93-105.

Rossor, A. M., Oates, E. C., Salter, H. K., Liu, Y., Murphy, S. M., Schule, R., Gonzalez, M. A., Scoto, M., Phadke, R., Sewry, C. A. et al. (2015). Phenotypic and molecular insights into spinal muscular atrophy due to mutations in BICD2. *Brain* **138**, 293-310.

Satoh, D., Sato, D., Tsuyama, T., Saito, M., Ohkura, H., Rolls, M. M., Ishikawa, F. and Uemura, T. (2008). Spatial control of branching within dendritic arbors by dynein-dependent transport of Rab5-endosomes. *Nat Cell Biol* **10**, 1164-71.

Schindelin, J., Arganda-Carreras, I., Frise, E., Kaynig, V., Longair, M., Pietzsch, T., Preibisch, S., Rueden, C., Saalfeld, S., Schmid, B. et al. (2012). Fiji: an open-source platform for biological-image analysis. *Nat Methods* **9**, 676-82.

Schmauss, C., Brines, M. L. and Lerner, M. R. (1992). The gene encoding the small nuclear ribonucleoprotein-associated protein N is expressed at high levels in neurons. *J Biol Chem* **267**, 8521-9.

Schrank, B., Gotz, R., Gunnersen, J. M., Ure, J. M., Toyka, K. V., Smith, A. G. and Sendtner, M. (1997). Inactivation of the survival motor neuron gene, a candidate gene for human spinal muscular atrophy, leads to massive cell death in early mouse embryos. *Proc Natl Acad Sci U S A* **94**, 9920-5.

Scoto, M., Rossor, A. M., Harms, M. B., Cirak, S., Calissano, M., Robb, S., Manzur, A. Y., Martinez Arroyo, A., Rodriguez Sanz, A., Mansour, S. et al. (2015). Novel mutations expand the clinical spectrum of DYNC1H1-associated spinal muscular atrophy. *Neurology* **84**, 668-79.

Shevchenko, A., Wilm, M., Vorm, O. and Mann, M. (1996). Mass spectrometric sequencing of proteins silver-stained polyacrylamide gels. *Anal Chem* **68**, 850-8.

Shinozaki, K., Kume, H., Kuzume, H., Obata, K. and Maruyama, K. (1999). Norbin, a neurite-outgrowth-related protein, is a cytosolic protein localized in the somatodendritic region of neurons and distributed prominently in dendritic outgrowth in Purkinje cells. *Brain Res Mol Brain Res* **71**, 364-8.

Shinozaki, K., Maruyama, K., Kume, H., Kuzume, H. and Obata, K. (1997). A novel brain gene, norbin, induced by treatment of tetraethylammonium in rat hippocampal slice and accompanied with neurite-outgrowth in neuro 2a cells. *Biochem Biophys Res Commun* **240**, 766-71.

Shpargel, K. B. and Matera, A. G. (2005). Gemin proteins are required for efficient assembly of Sm-class ribonucleoproteins. *Proc Natl Acad Sci U S A* **102**, 17372-7.

Singh, R. N., Howell, M. D., Ottesen, E. W. and Singh, N. N. (2017). Diverse role of survival motor neuron protein. *Biochim Biophys Acta* **1860**, 299-315.

Sleeman, J. (2013). Small nuclear RNAs and mRNAs: linking RNA processing and transport to spinal muscular atrophy. *Biochem Soc Trans* **41**, 871-5.

Sleeman, J. E., Ajuh, P. and Lamond, A. I. (2001). snRNP protein expression enhances the formation of Cajal bodies containing p80-coilin and SMN. *J Cell Sci* **114**, 4407-19.

Sleeman, J. E. and Lamond, A. I. (1999). Newly assembled snRNPs associate with coiled bodies before speckles, suggesting a nuclear snRNP maturation pathway. *Curr Biol* **9**, 1065-74.

Sleeman, J. E., Trinkle-Mulcahy, L., Prescott, A. R., Ogg, S. C. and Lamond, A. I. (2003). Cajal body proteins SMN and Coilin show differential dynamic behaviour in vivo. *J Cell Sci* **116**, 2039-50.

Sleigh, J. N., Gillingwater, T. H. and Talbot, K. (2011). The contribution of mouse models to understanding the pathogenesis of spinal muscular atrophy. *Dis Model Mech* **4**, 457-67.

Stark, H., Dube, P., Luhrmann, R. and Kastner, B. (2001). Arrangement of RNA and proteins in the spliceosomal U1 small nuclear ribonucleoprotein particle. *Nature* **409**, 539-42.

Strickland, A. V., Schabhuttl, M., Offenbacher, H., Synofzik, M., Hauser, N. S., Brunner-Krainz, M., Gruber-Sedlmayr, U., Moore, S. A., Windhager, R., Bender, B. et al. (2015). Mutation screen reveals novel variants and expands the phenotypes associated with DYNC1H1. *J Neurol* **262**, 2124-34.

Synofzik, M., Martinez-Carrera, L. A., Lindig, T., Schols, L. and Wirth, B. (2014). Dominant spinal muscular atrophy due to BICD2: a novel mutation refines the phenotype. *J Neurol Neurosurg Psychiatry* **85**, 590-2.

Takaku, M., Tsujita, T., Horikoshi, N., Takizawa, Y., Qing, Y., Hirota, K., Ikura, M., Ikura, T., Takeda, S. and Kurumizaka, H. (2011). Purification of the human SMN-GEMIN2 complex and assessment of its stimulation of RAD51-mediated DNA recombination reactions. *Biochemistry* **50**, 6797-805.

Ting, C. H., Wen, H. L., Liu, H. C., Hsieh-Li, H. M., Li, H. and Lin-Chao, S. (2012). The spinal muscular atrophy disease protein SMN is linked to the Golgi network. *PLoS One* **7**, e51826.

Tisdale, S., Lotti, F., Saieva, L., Van Meerbeke, J. P., Crawford, T. O., Sumner, C. J., Mentis, G. Z. and Pellizzoni, L. (2013). SMN is essential for the biogenesis of U7 small nuclear ribonucleoprotein and 3'-end formation of histone mRNAs. *Cell Rep* **5**, 1187-95.

Tisdale, S. and Pellizzoni, L. (2015). Disease mechanisms and therapeutic approaches in spinal muscular atrophy. *J Neurosci* **35**, 8691-700.

Todd, A. G., Morse, R., Shaw, D. J., McGinley, S., Stebbings, H. and Young, P. J. (2010a). SMN, Gemin2 and Gemin3 associate with beta-actin mRNA in the cytoplasm of neuronal cells in vitro. *J Mol Biol* **401**, 681-9.

Todd, A. G., Morse, R., Shaw, D. J., Stebbings, H. and Young, P. J. (2010b). Analysis of SMN-neurite granules: Core Cajal body components are absent from SMN-cytoplasmic complexes. *Biochem Biophys Res Commun* **397**, 479-85.

Trinkle-Mulcahy, L., Boulon, S., Lam, Y. W., Urcia, R., Boisvert, F. M., Vandermoere, F., Morrice, N. A., Swift, S., Rothbauer, U., Leonhardt, H. et al. (2008). Identifying specific protein interaction partners using quantitative mass spectrometry and bead proteomes. *J Cell Biol* **183**, 223-39.

Tsurusaki, Y., Saitoh, S., Tomizawa, K., Sudo, A., Asahina, N., Shiraishi, H., Ito, J., Tanaka, H., Doi, H., Saitsu, H. et al. (2012). A DYNC1H1 mutation causes a dominant spinal muscular atrophy with lower extremity predominance. *Neurogenetics* **13**, 327-32.

Urlaub, H., Raker, V. A., Kostka, S. and Luhrmann, R. (2001). Sm protein-Sm site RNA interactions within the inner ring of the spliceosomal snRNP core structure. *EMBO J* **20**, 187-96.

Vizcaino, J. A., Csordas, A., Del-Toro, N., Dianes, J. A., Griss, J., Lavidas, I., Mayer, G., Perez-Riverol, Y., Reisinger, F., Ternent, T. et al. (2016). 2016 update of the PRIDE database and its related tools. *Nucleic Acids Res* **44**, 11033.

Vonderheit, A. and Helenius, A. (2005). Rab7 associates with early endosomes to mediate sorting and transport of Semliki forest virus to late endosomes. *PLoS Biol* **3**, e233.

Wan, L., Battle, D. J., Yong, J., Gubitz, A. K., Kolb, S. J., Wang, J. and Dreyfuss, G. (2005). The survival of motor neurons protein determines the capacity for snRNP assembly: biochemical deficiency in spinal muscular atrophy. *Mol Cell Biol* **25**, 5543-51.

Wang, H., Duan, X., Ren, Y., Liu, Y., Huang, M., Liu, P., Wang, R., Gao, G., Zhou, L., Feng, Z. et al. (2013). FoxO3a negatively regulates nerve growth factor-induced neuronal differentiation through inhibiting the expression of neurochondrin in PC12 cells. *Mol Neurobiol* **47**, 24-36.

Wang, H., Westin, L., Nong, Y., Birnbaum, S., Bendor, J., Brismar, H., Nestler, E., Aperia, A., Flajolet, M. and Greengard, P. (2009). Norbin is an endogenous regulator of metabotropic glutamate receptor 5 signaling. *Science* **326**, 1554-7.

Ward, R. J., Jenkins, L. and Milligan, G. (2009). Selectivity and functional consequences of interactions of family A G protein-coupled receptors with neurochondrin and periplakin. *J Neurochem* **109**, 182-92.

Winkler, C., Eggert, C., Gradl, D., Meister, G., Giegerich, M., Wedlich, D., Laggerbauer, B. and Fischer, U. (2005). Reduced U snRNP assembly causes motor axon degeneration in an animal model for spinal muscular atrophy. *Genes Dev* **19**, 2320-30.

Wishart, T. M., Mutsaers, C. A., Riessland, M., Reimer, M. M., Hunter, G., Hannam, M. L., Eaton, S. L., Fuller, H. R., Roche, S. L., Somers, E. et al. (2014). Dysregulation of ubiquitin homeostasis and beta-catenin signaling promote spinal muscular atrophy. *J Clin Invest* **124**, 1821-34.

Xiong, X. P., Vogler, G., Kurthkoti, K., Samsonova, A. and Zhou, R. (2015). SmD1 Modulates the miRNA Pathway Independently of Its Pre-mRNA Splicing Function. *PLoS Genet* **11**, e1005475.

Zhang, H., Xing, L., Rossoll, W., Wichterle, H., Singer, R. H. and Bassell, G. J. (2006). Multiprotein complexes of the survival of motor neuron protein SMN with Gemins traffic to neuronal processes and growth cones of motor neurons. *J Neurosci* **26**, 8622-32.

Zhang, H. L., Pan, F., Hong, D., Shenoy, S. M., Singer, R. H. and Bassell, G. J. (2003). Active transport of the survival motor neuron protein and the role of exon-7 in cytoplasmic localization. *J Neurosci* **23**, 6627-37.

Zhang, Z., Lotti, F., Dittmar, K., Younis, I., Wan, L., Kasim, M. and Dreyfuss, G. (2008). SMN deficiency causes tissue-specific perturbations in the repertoire of snRNAs and widespread defects in splicing. *Cell* **133**, 585-600.

Zhao, D. Y., Gish, G., Braunschweig, U., Li, Y., Ni, Z., Schmitges, F. W., Zhong, G., Liu, K., Li, W., Moffat, J. et al. (2016). SMN and symmetric arginine dimethylation of RNA polymerase II C-terminal domain control termination. *Nature* **529**, 48-53.

Zou, J., Barahmand-pour, F., Blackburn, M. L., Matsui, Y., Chansky, H. A. and Yang, L. (2004). Survival motor neuron (SMN) protein interacts with transcription corepressor mSin3A. *J Biol Chem* **279**, 14922-8.

Zou, T., Yang, X., Pan, D., Huang, J., Sahin, M. and Zhou, J. (2011). SMN deficiency reduces cellular ability to form stress granules, sensitizing cells to stress. *Cell Mol Neurobiol* **31**, 541-50.

Figures

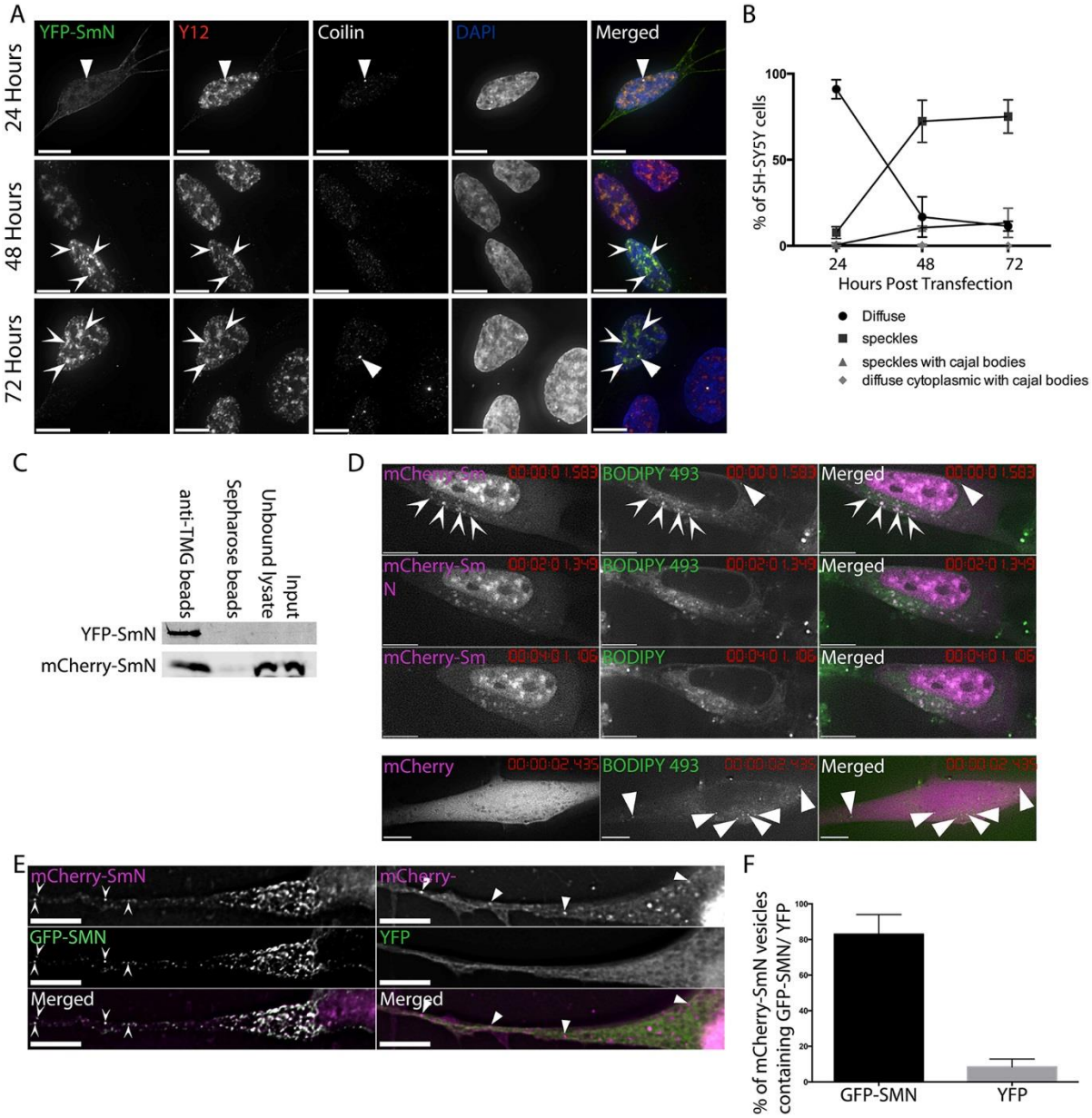

Figure 1: SmN exhibits similar behaviour to SmB in SH-SY5Y cells. A) SH-SY5Y cells transiently expressing YFP-SmN and fixed after 24, 48 and 72 hours show variations in distribution of the YFP-SmN with time. Immunostaining with Y12 (red on overlay) and anti-coilin (white on overlay) shows splicing speckles (arrowheads) and Cajal Bodies (CBs, triangles) respectively. Images are deconvolved z-stacks with 0.2 μm spacing. Bar=7μm. B) SmN initially localises diffusely in the cytoplasm, before localising to speckles at the 48 and 72 hour time-points. 3 independent experiments, n=100 cells per experiment. Data shown is mean +/- SD). C) Western blot analysis of

snRNPs immunprecipitated using TMG beads (left hand lane) confirms that both YFP-SmN (detected with anti-YFP, top row) and mCherry-SmN (detected with anti-mCherry, bottom row) are incorporated into snRNPs. D) mCherry-SmN cytoplasmic structures are mobile and stain with the lipophilic dye BODIPY 493. Arrows identify mCherry-SmN structures stained with BODIPY 493, triangles identify BODIPY 493-stained vesicles not containing mCherry-SmN. mCherry alone does not accumulate in BODIPY 493-stained vesicles. Cells were imaged approximately every 4 seconds for 9 minutes. Images are single deconvolved z-sections. Bar=7μm. E) mCherry-SmN and GFP-SMN co-localise in cytoplasmic foci in SH-SY5Y cells (arrowheads in left hand panels), whereas YFP alone shows no accumulation in mCherry-SmN foci (triangles in right hand panels). White signal on the overlay indicates areas of co-localisation. Images are single deconvolved z-sections. Bar=7μm. F) Comparison of the percentage of mCherry-SmN vesicles per cell co-localising with GFP-SMN to those showing co-incidental overlap with YFP alone confirms the co-localisation (unpaired 2 tailed t-test, p=<0.0001, n=5).

A

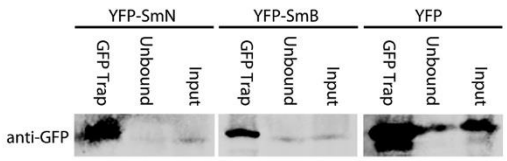

B

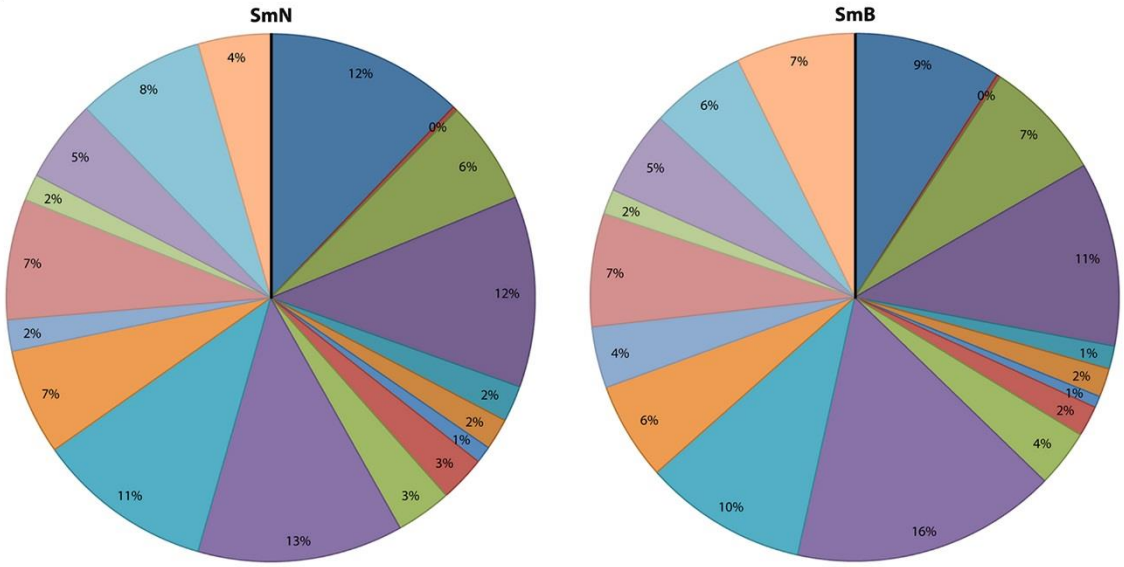

	% of total proteins identified	
	SmN	SmB
Splicing and snRNP assembly	12.1%	9.0%
Methylosome	0.3%	0.2%
Vesicle transport	6.4%	7.4%
Signal transduction	11.7%	11.3%
Neural proteins	2.2%	1.4%
Apoptosis	1.9%	1.8%
Motor Proteins	1.0%	0.7%
Cytoskeletal related proteins	2.8%	1.9%
Mitochondria	3.4%	3.5%
Metabolism and synthesis	12.6%	16.2%
DNA replication and repair	10.8%	10.0%
Transcription	6.5%	6.0%
Post-translation modification	1.9%	3.8%
RNA interacting/processing	7.4%	6.9%
RNA degradation	1.6%	1.5%
Proteolysis	5.0%	5.2%
Unknown	7.8%	5.9%
Other	4.4%	7.3%

D

```
SmB:  MTVGKSSKMLQHIDYRMRCILQDGRIFIGTFKAFDKHMNLILCDCDEFRKIKPKN
SmN:  MTVGKSSKMLQHIDYRMRCILQDGRIFIGTFKAFDKHMNLILCDCDEFRKIKPKN

SmB:  SKQAEREEKRVLGLVLLRGENLVSMTVEGPPPKDTGIARVPLAGAAGGPGIGRAA
SmN:  AKQPEREEKRVLGLVLLRGENLVSMTVEGPPPKDTGIARVPLAGAAGGPGVGRAA

SmB:  GRGIPAGVPMPQAPAGLAGPVRGVGGPSQQVMTPQGRGTVAAAAAATASIAGAP
SmN:  GRGVPAGVPIPQAPAGLAGPVRGVGGPSQQVMTPQGRGTVAAAAVAATASIAGAP

SmB:  TQYPPGRGGPPPPMGRGAPPPGMMGPPPGMRPPMGPPMGIPPGRGTPMGMPPPGM
SmN:  TQYPPGRGTPPPPVGRATPPPGIMAPPPGMRPPMGPPIGLPPARGTPIGMPPPGM

SmB:  RPPPPGMRGLL
SmN:  RPPPPGIRGPPPPGMRPPRP
```

C

Sequence	Scaffold Peptide Identification Probability	Mascot Ion Score	Mascot Identity Score	Mascot Delta Ion Score	Observed Mass	Actual Mass	Charge	Δ Dalton	Δ PPM
(R)IFDAVGFTFPNR(L)	100%	45.4	35.1	38.3	692.35	1382.68	2	-0.0140	-10.00
(K)IPILSTFLTAR(G)	100%	56.5	31.7	50.4	616.37	1230.72	2	-0.0150	-12.00
(R)LALEETGTEVK(E)	100%	47.1	36.6	47.1	595.32	1188.62	2	-0.0079	-6.60
(R)LLSTSPALQGTPASR(G)	100%	111.1	34.8	98.9	749.90	1497.79	2	-0.0200	-14.00
(R)LQAGEETASHYR(M)	100%	75.1	34.3	75.1	454.55	1360.63	3	-0.0049	-3.60

Figure 2: The interactomes of SmB and SmN are similar, but there are differences at the level of individual proteins. A) Immunoblot analysis confirms efficient affinity purification of YFP-SmN, YFP-SmB and YFP. 10% of the affinity purified material (left hand lane in each panel) was compared to 80μg of precleared lysate (Input) and unbound material using anti-GFP. GFP-Trap effectively immunoprecipitated all three proteins. B) After processing the mass spectrometry data,

and sorting identified proteins into groups based on Gene Ontology annotations, the interactomes of SmN and SmB are very similar. C) A comparison between the amino acid sequences of SmN and SmB reveals their similarity. Differences in amino acid sequence are in red. Sequences were from Uniprot (entries P63162 (SmN) and P14678-2 (SmB)). D) Neurochondrin (NCDN) was identified in the interactome of YFP-SmN, with 5 unique peptide hits encompassing 9% sequence coverage. Each Ion score (Mascot Ion Score) was above the threshold for peptide identity (Mascot Identity Score), with 2 out of the 5 identified peptides having a score of above double the threshold score.

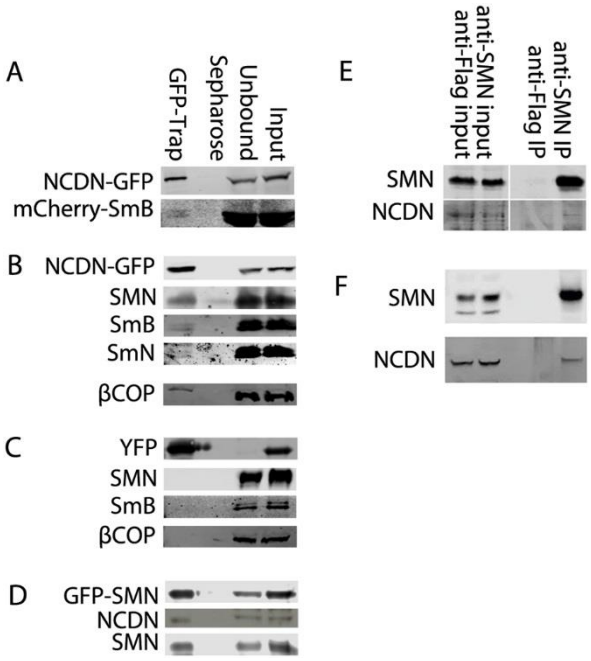

Figure 3: NCDN interacts with SmN, SmB and SMN in cell lines and in vivo A) Affinity isolation of NCDN-GFP using GFP-Trap, detected with anti-GFP (top row) co-enriches mCherry-SmB, detected with anti-mCherry (bottom row) in transiently co-transfected SH-SY5Y cells B) In an SH-SY5Y cell line constitutively expressing NCDN-GFP, affinity isolation of NCDN-GFP, detected with anti-GFP (top row) co-enriches SMN, SmB, SmN and the Coatomer protein βCOP, all detected with antibodies against the endogenous proteins (as labelled). C) In an SH-SY5Y cell line constitutively expressing YFP, affinity isolation of YFP, detected with anti-GFP (top row) does not co-enrich SMN, SmB or βCOP, all detected with antibodies to the endogenous proteins (as labelled). D) In an SH-SY5Y cell line constitutively expressing GFP-SMN, affinity isolation of GFP-SMN, detected with anti-GFP (top row) co-enriches endogenous NCDN, detected with anti-NCDN (middle row). Endogenous SMN, detected with anti-SMN (bottom row) is also co-enriched. E) Immunoprecipitation of endogenous SMN co-enriches endogenous NCDN in SH-SY5Y cells. F) Immunoprecipitation of endogenous SMN from murine P8 brain lysate co-enriches NCDN.

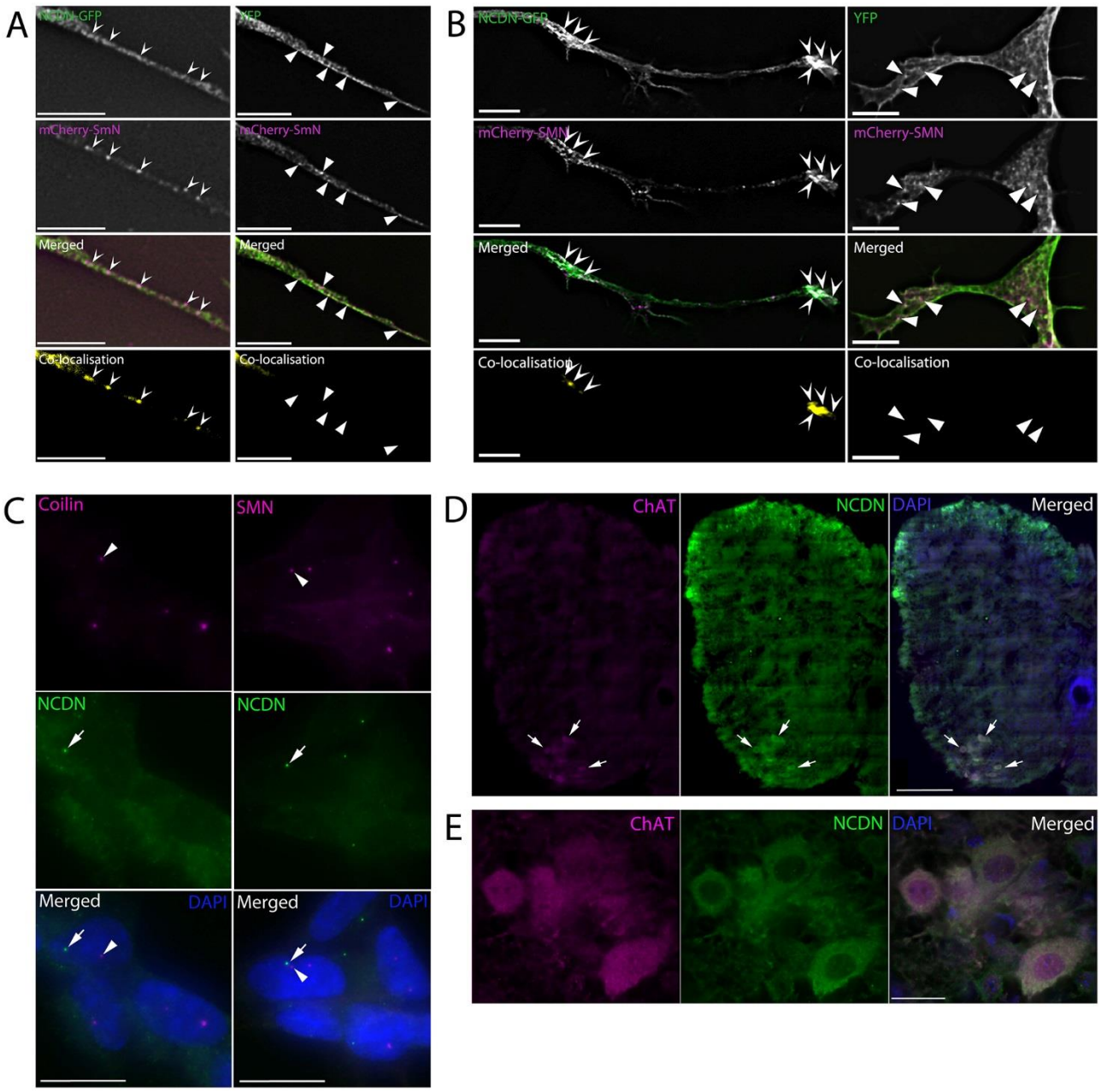

Figure 4: NCDN colocalises with SmN and SMN in the cytoplasm but not the nucleus and is expressed in motor neurones in mouse spinal cord. A) NCDN-GFP and mCherry-SmN co-localise in vesicle-like structures (arrows) in neurites of SH-SY5Y cells constitutively expressing mCherry-SmN, and transiently expressing NCDN-GFP (left hand panels). White areas in the merged image show areas of co-localisation. Co-localisation images (bottom row) were generated in Volocity, using automatic thresholds on undeconvolved z-sections before excluding values below 0.05 (see material and methods). No co-localisation is seen in the same cell line transiently expressing YFP alone (right hand panel). Triangles show structures containing mCherry-SmN, but not YFP. B) mCherry-SMN and NCDN-GFP co-localise in vesicles (arrows) in the cytoplasm of co-transfected

SH-SY5Y cells (left hand panels). White areas in the merged image show areas of co-localisation. Co-localisation images (bottom row) were generated as above. No co-localisation is observed between mCherry-SMN and YFP (triangles, right hand panels). Bar= 7μm. C) NCDN forms nuclear foci (arrows) in the nuclei of a small proportion of SH-SY5Y cells (≤2%, 2 independent experiments, n=100 cells per experiment). These do not co-localise with nuclear foci stained with coilin (arrowheads, left hand panels) or SMN (arrowheads, right hand panels). D) NCDN (green) is expressed throughout the spinal cord, with increased expression in motor neurons (arrows), identified with anti-ChAT (magenta). Bar=500μm. E) Higher magnification imaging confirms the presence of NCDN in ChAT-positive motor neurones (single deconvolved z-section). Bar=10μm.

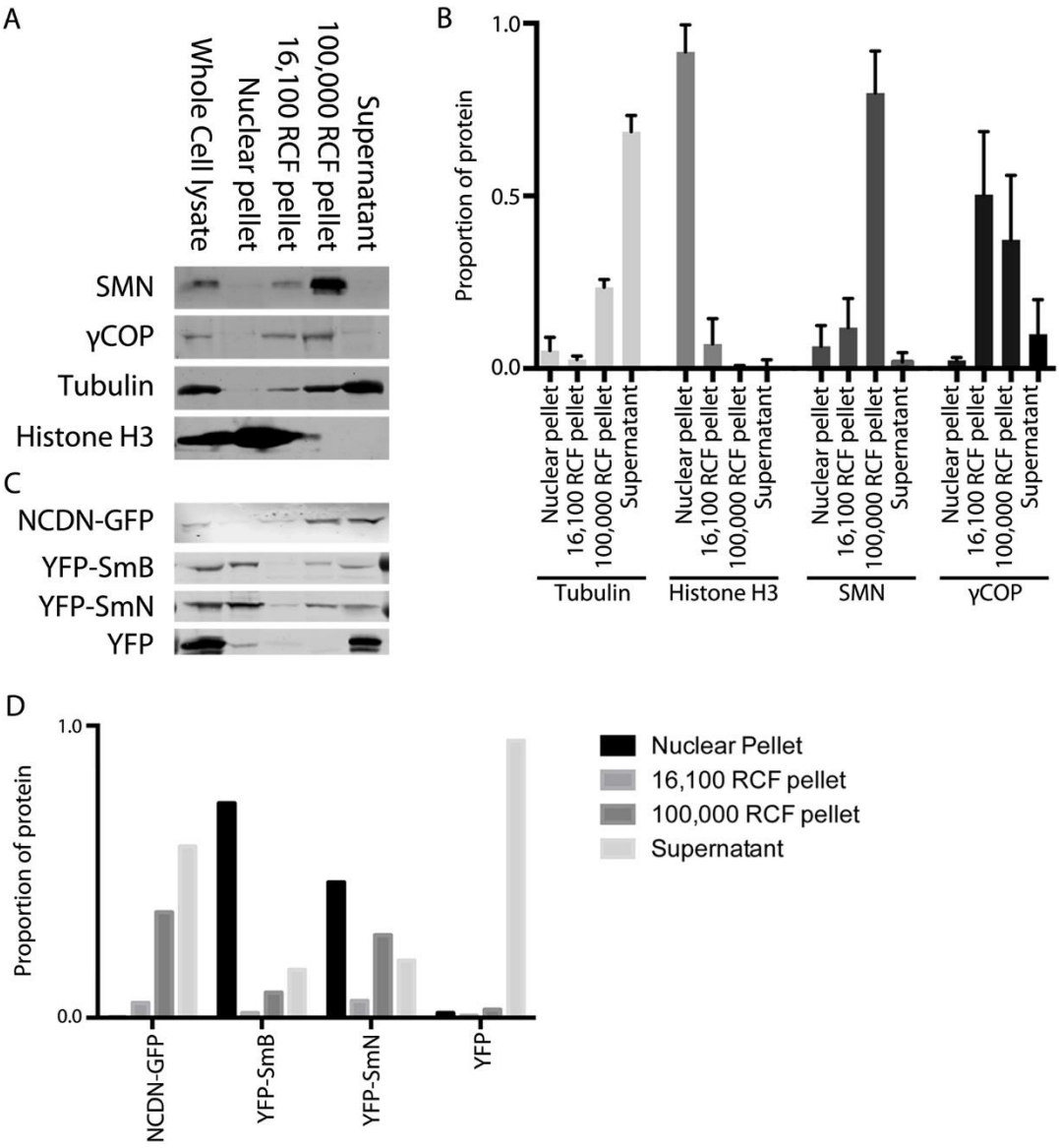

Figure 5: Detergent-free fractionation of SH-SY5Y cells reveals that SMN, coatomer proteins, NCDN, SmB and SmN are all enriched in the 100,000 RCF vesicle pellet. A) Immunoblotting of equal protein amounts from fractionated SH-SY5Y cells reveals that SMN (top row) is highly enriched in the 100,000 RCF pellet, with smaller amounts seen in the 16,100 RCF pellet and the nuclear pellet. The coatomer protein, γCOP (second row) is also enriched in the 100,00 RCF pellet as well as the 16,100 RCF pellet. Antibodies to histone H3 and tubulin confirm minimal nuclear contamination in cytoplasmic fractions, and minimal cytoplasmic contamination in the nuclear pellet, respectively. B) Quantitation of immunoblot analysis confirms that SMN is highly enriched in the 100,000 RCF pellet, with enrichment of γCop also seen. Histone H3 and tubulin are highly enriched in the nucleus and cytoplasm respectively. Quantitation of tubulin and histone H3 bands was from 7 immunoblots, with values from SMN and γCOP from 5 and 4 immunoblots

respectively. C) Immunoblotting of equal protein amounts from fractionated SH-SY5Y cells constitutively expressing NCDN-GFP, YFP-SmB, YFP-SmN or YFP alone (all detected with anti-GFP) reveals that NCDN-GFP is enriched in the 100,000 RCF pellet, with smaller amounts seen in the 16,100 RCF pellet and the cytosolic supernatant. YFP-SmB and YFP-SmN are both also found in the 100,000 RCF pellet, in addition to the nuclear pellet and cytosolic supernatant. YFP alone is found almost exclusively in the cytosolic supernatant, with none detected in the 100,000 RCF or 16,100 RCF pellets. D) Quantitation of the immunoblots in C) confirms the presence of NCDN-GFP, YFP-SmB and YFP-SmN in the 100,000 RCF pellet, together with the restriction of YFP alone to the residual cytosolic supernatant.

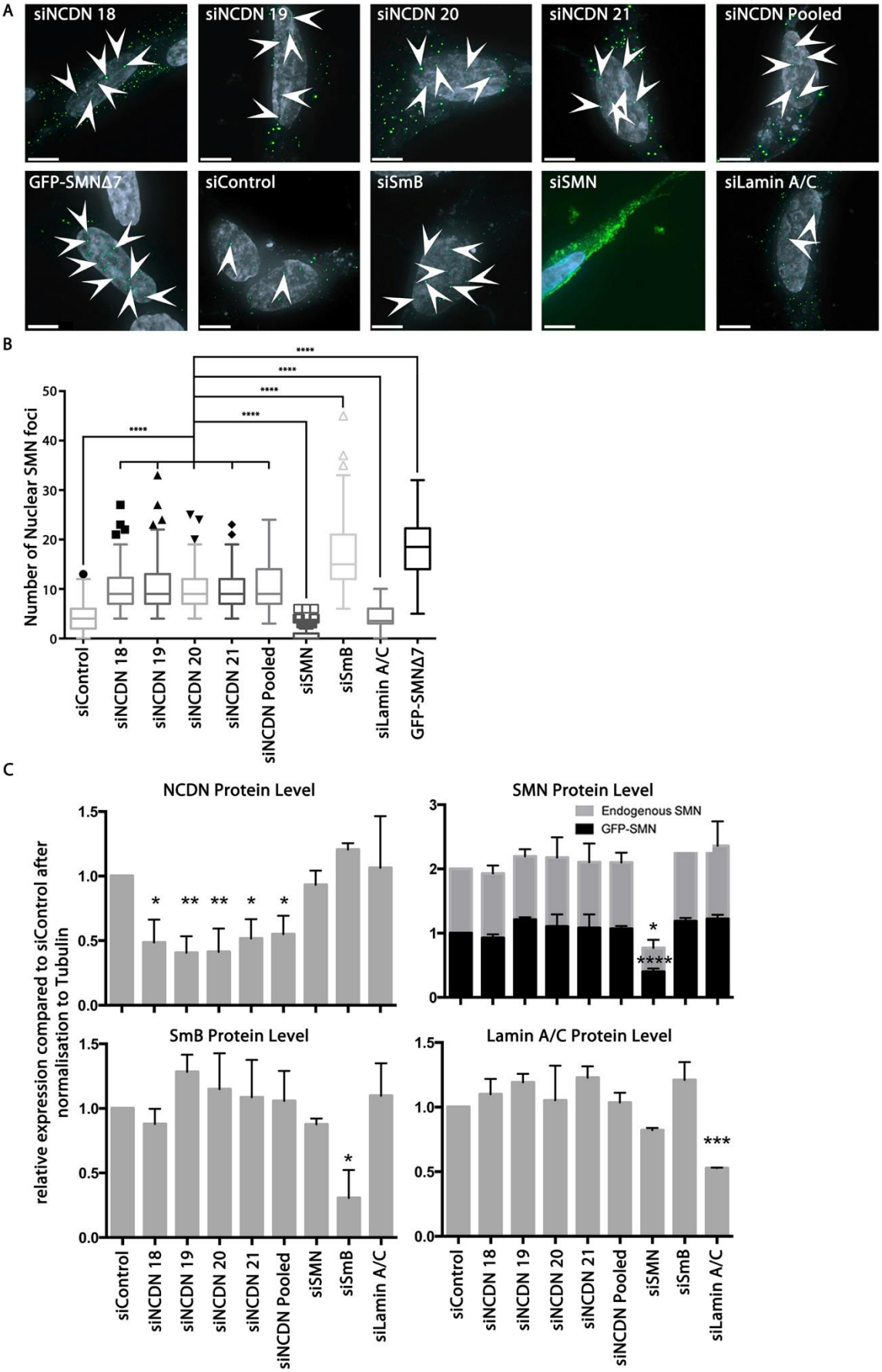

Figure 6: Reduction of endogenous NCDN using siRNA increases localisation of SMN to nuclear foci. A) Transfection of SH-SY5Y cells constitutively expressing GFP-SMN (Green) with siRNAs shows an increase in the number of SMN-positive nuclear foci (arrows) in cells transfected with siRNAs against NCDN or SmB and a decrease in the number of SMN-positive nuclear foci in cells transfected with siRNAs against SMN in comparison to cells transfected with non-targeting siRNAs (siControl) or siRNAs against lamin A/C as a 'targeting' control. Transfection of SH-SY5Y cells with a plasmid to express GFP-SMNΔ7 also results in increased numbers of SMN-positive nuclear foci. Cell nuclei are stained with Hoescht 33342 (grey on images). Transfection efficiency with siRNAs was greater than 90%, measured by transfection with siGlo Cyclophillin B (not shown). Bar=7μm. Images are deconvolved z-stacks taken with 0.2μm spacing B) Quantitation of numbers of SMN-positive nuclear foci per nucleus shows a significant increase following reduction of NCDN (10.2 (± 4.1) with siNCDN 18, 10.4 (± 4.9)) (Mean ± Standard Deviation) with siNCDN 19, 9.9 (± 4.1) with siNCDN 20, 9.5 (± 3.6) with siNCDN 21 and 10.7 (± 4.6) with siNCDN pooled compared to 4.4 (± 2.5) in cells treated with non-targeting siRNA (siControl) and 4.2 (± 2.3) in cells treated with siRNAs targeting lamon A/C (siLaminA/C) . Reduction of SmB also shows an increase in numbers of SMN-positive nuclear foci (to 16.7 (± 6.8) with siSmB), while reduction of SMN leads to a decrease in numbers of SMN-positive nuclear foci (to 0.7 (± 1.4) with siSMN). Expression of GFP-SMNΔ7 results in an increase of numbers of SMN-positive nuclear foci to 18.2 (± 5.3). The difference between each siNCDN and controls is statistically significant (AVOVA; $P<0.0001$, n=150 from 3 replicates). A Tukey post-test identified outliers (individual points marked on graph). C) Immunoblot analysis using antibodies to endogenous NCDN, SMN and SmB shows a reduction in expression of each of 40-60% compared to siControl cells, after signals were normalised to tubulin (see also Fig. S5). Reductions in protein expression compared to siControl siRNA are statistically significant (ANOVA; $P<0.0001$ for NCDN, Lamin A/C and endogenous SMN, $P<0.001$ for SmB, and $P<0.01$ for GFP-SMN, n=3). A Dunnett post-test identified the significance of the reduction compared to siControl.

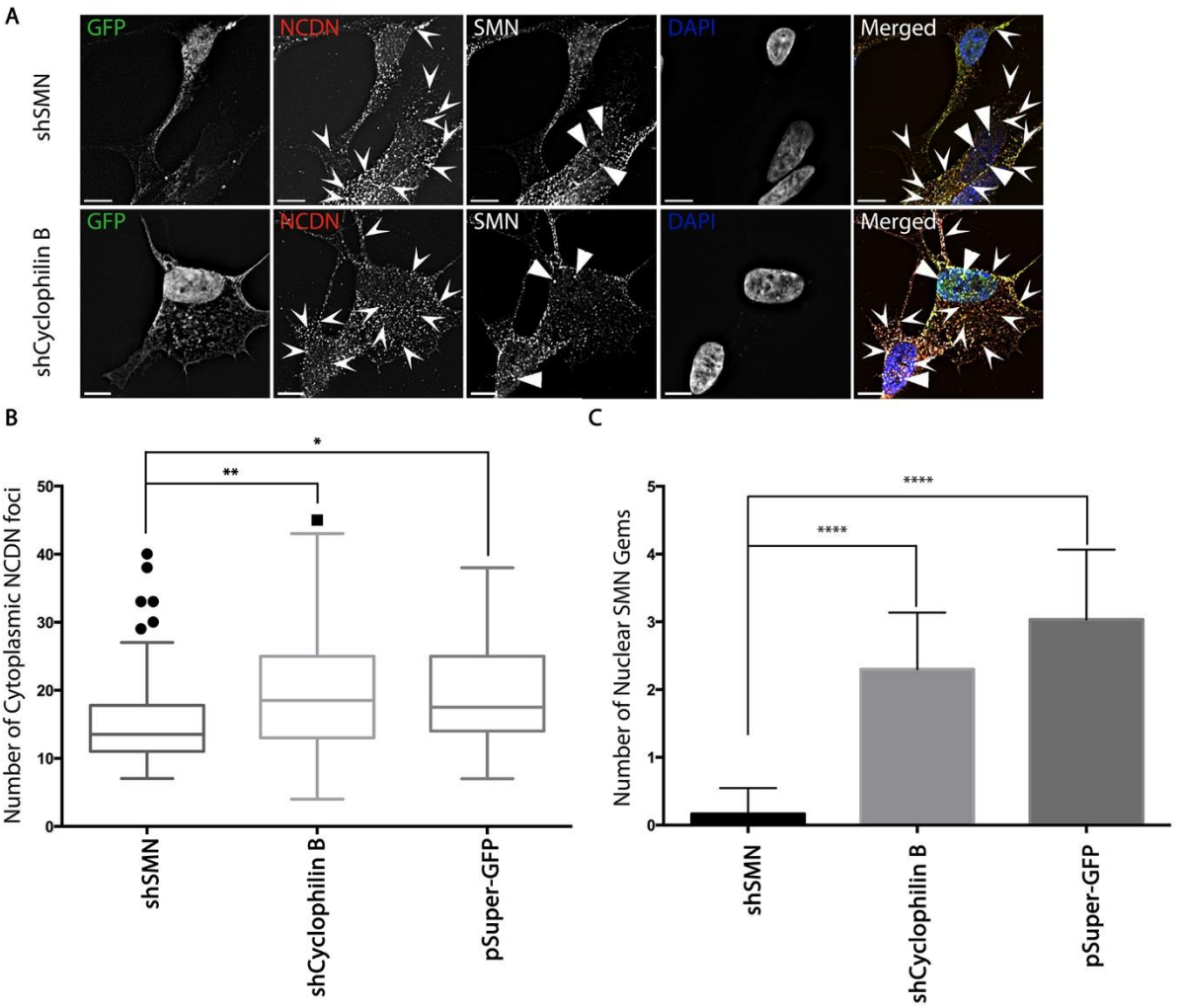

Figure 7: Reduction of endogenous SMN causes a reduction in cytoplasmic NCDN foci in SH-SY5Y cells. A) SH-SY5Y cells were transfected with plasmids to express shRNAs targeting SMN (shSMN), Cyclophilin B (shCyclophilin) or with the empty pSuper GFP vector (not shown), fixed after 72 hours, and immunostained for endogenous NCDN and SMN allowing detection of NCDN foci within the cytoplasm (arrowheads), as well as SMN-positive nuclear gems (identified with Triangles). Bar= 7μm, images are single deconvolved z-sections B) The depletion of SMN results in a reduction in the number of NCDN foci present in the cytoplasm to 15.3 (± 7.2) (Mean ± Standard Deviation) from 20.6 (± 12.0) and 19.5 (± 7.6) compared to cells transfected with either shCyclophilin B or the empty pSuper GFP vector respectively (ANOVA P<0.0005, n=64 from 3 replicates). C) The depletion of SMN causes a reduction of nuclear gems to 0.17 (± 0.38) from 2.3 (± 0.84) or 3.0 (± 1.0) compared to cells transfected with shCyclophilin B or empty vector respectively confirming efficient reduction in SMN protein levels (ANOVA P<0.0001, n=30 from 3 replicates).

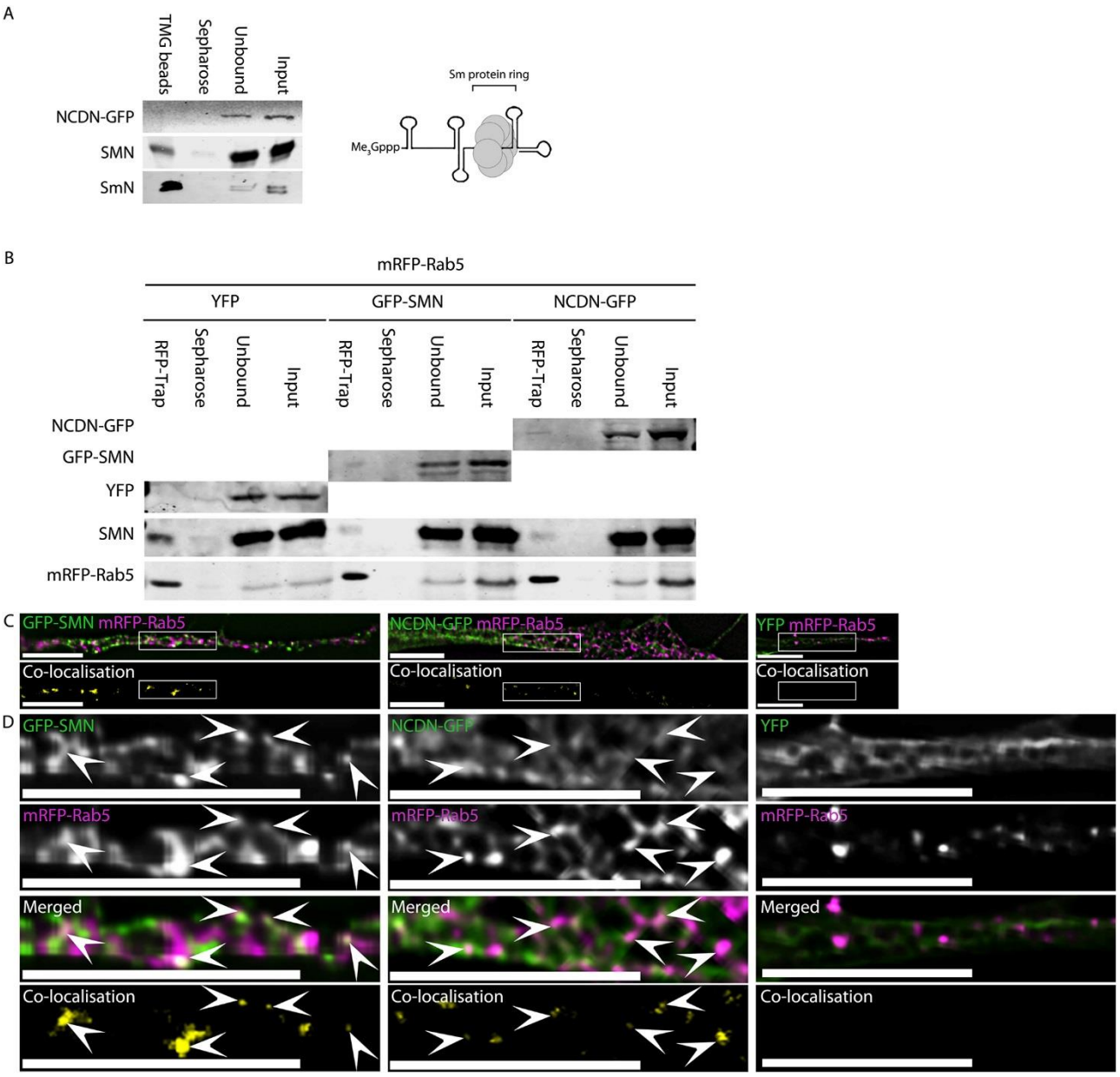

Figure 8: NCDN does not co-purify with snRNPs, while NCDN and SMN interact with Rab5 and co-localise with a subset of Rab5 vesicles within neurites of SH-SY5Y cells. A) Incubation of whole-cell lysate from an SH-SY5Y cell line constitutively expressing NCDN-GFP with agarose beads conjugated to antibodies against the tri-methyl guanosine cap (Me3Gppp) of snRNAs (TMG beads) affinity purifies snRNPs as evidenced by the enrichment of the core snRNP protein SmN (detected with anti-SmN, bottom row). The enriched snRNP fraction also contains SMN, which is essential for snRNP assembly. NCDN-GFP, however, does not co-enrich with snRNPs. Also shown is the core structure of mature snRNPs consisting of the heptameric Sm protein ring bound at the Sm binding site of snRNA, as well as the characteristic tri-methyl guanosine Cap of snRNAs (Me_3Gppp) at the 5' end. B) Affinity isolation of mRFP-Rab5 using RFP-Trap from cells co-transfected with

plasmids to express mRFP-Rab5 together with NCDN-GFP, GFP-SMN or YFP alone co-enriches both NCDN-GFP (top row, detected with anti-GFP, band is present in RFP-Trap lane but not sepharose beads lane) and SMN-GFP (second row, detected with anti-GFP, band is present in RFP-Trap lane but not sepharose beads lane), but not YFP (third row, no band detected in RFP-Trap lane). Endogenous SMN (fourth row, detected with mouse anti-SMN) co-enriches with mRFP-Rab5 in all three samples. Detection of mRFP-Rab5 (bottom row, detected with anti-RFP) confirms robust enrichment of mRFP-Rab5 in all three samples. C) Both GFP-SMN and NCDN-GFP partially co-localise with mRFP-Rab5 in a subset of mRFP-Rab5 containing vesicles in co-transfected SH-SY5Y cells (white signal in overlaid images, top row; yellow signal in co-localisation images, bottom row). D) Enlargement of the boxed areas in C) confirms that the co-localisation between SMN/NCDN and Rab5 occurs in punctate structures. Arrowheads identify areas of co-localisation. Co-localisation images were generated by Volocity, using automatic thresholds on non-deconvolved z-sections before excluding values below 0.05. Images (excluding the co-localisation images) are single deconvolved z-sections. Bar=7μm.

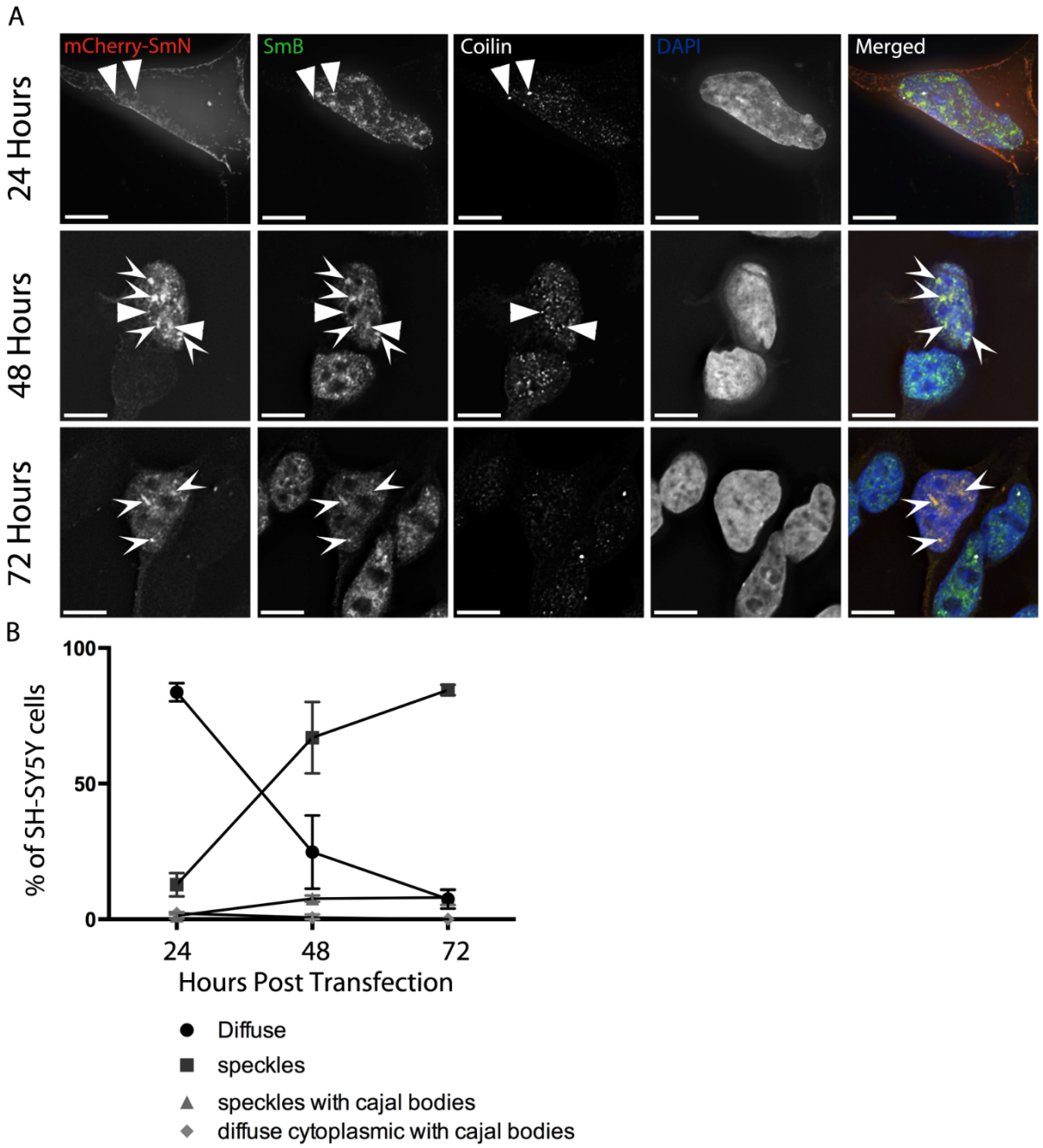

Figure S1: mCherry-SmN exhibits similar behaviour to both YFP-SmN and SmB in SH-SY5Y cells. A) SH-SY5Y cells transiently expressing mCherry-SmN and fixed after 24, 48 and 72 hours show variations in distribution of the mCherry-SmN with time. Immunostaining with Y12 (green on overlay) and anti-coilin (white on overlay) shows splicing speckles (arrowheads) and Cajal Bodies (CBs, triangles) respectively. Images are deconvolved z-stacks with 0.2 μm spacing. Bar=7μm. B) mCherry-SmN initially localises diffusely in the cytoplasm, before localising to speckles at the 48 and 72 hour time-points. 3 independent experiments, n=100 cells per experiment. Data shown is mean ± SD.

Identified protein	Accession number	Molecular Weight	SmN	SmB	YFP
small nuclear ribonucleoprotein polypeptide B * [Homo sapiens]	gi|53690154	24 kDa	13	11	2
small nuclear ribonucleoprotein Sm D2 isoform 1 [Homo sapiens]	gi|4759158	14 kDa	10	8	4
small nuclear ribonucleoprotein Sm D1 [Homo sapiens]	gi|5902102	13 kDa	5	5	4
small nuclear ribonucleoprotein E [Homo sapiens]	gi|4507129	11 kDa	5	4	2
small nuclear ribonucleoprotein F [Homo sapiens]	gi|4507131	10 kDa	5	3	0
small nuclear ribonucleoprotein Sm D3 [Homo sapiens]	gi|4759160	14 kDa	4	4	3
small nuclear ribonucleoprotein G [Homo sapiens]	gi|4507133	8 kDa	4	3	0
survival motor neuron protein isoform a [Homo sapiens]	gi|13259527	30 kDa	8	7	0
GEMIN5 protein [Homo sapiens]	gi|219517971	168 kDa	22	25	0
HC56 (Gemin 4) [Homo sapiens]	gi|10945430	119 kDa	18	11	0
DEAD box RNA helicase Gemin3 [Homo sapiens]	gi|6503002	92 kDa	12	18	0
gem-associated protein 2 isoform alpha [Homo sapiens]	gi|4506961	32 kDa	6	4	0
gem-associated protein 8 [Homo sapiens]	gi|8923481	29 kDa	6	2	0
Gem (nuclear organelle) associated protein 6 [Homo sapiens]	gi|17390437	19 kDa	3	3	0
gem-associated protein 7 [Homo sapiens]	gi|13376001	15 kDa	3	2	0
WD-40 repeat protein (Unrip) [Homo sapiens]	gi|4519417	38 kDa	16	16	0
U6 snRNA-associated Sm-like protein LSm4 isoform 1 [Homo sapiens]	gi|6912486	15 kDa	5	4	0
U6 snRNA-associated Sm-like protein LSm2 [Homo sapiens]	gi|10863977	11 kDa	4	4	0
U6 snRNA-associated Sm-like protein LSm6 [Homo sapiens]	gi|5901998	9 kDa	2	2	0
U6 snRNA-associated Sm-like protein LSm3 [Homo sapiens]	gi|7657315	12 kDa	2	2	0
U6 snRNA-associated Sm-like protein LSm7 [Homo sapiens]	gi|7706423	12 kDa	2	0	0
U7 snRNA-associated Sm-like protein LSm11 [Homo sapiens]	gi|27735089	40 kDa	2	0	0
protein arginine N-methyltransferase 5 isoform a [Homo sapiens]	gi|20070220	73 kDa	30	31	3
methylosome protein 50 [Homo sapiens]	gi|13129110	37 kDa	12	10	0
methylosome subunit pICln [Homo sapiens]	gi|4502891	26 kDa	7	8	0
CD2 antigen cytoplasmic tail-binding protein 2 [Homo sapiens]	gi|5174409	38 kDa	13	12	0
PERQ amino acid-rich with GYF domain-containing protein 2 isoform c [Homo sapiens]	gi|156766047	149 kDa	2	4	0
WW domain-binding protein 4 [Homo sapiens]	gi|6005948	43 kDa	3	0	0
formin binding protein 4, isoform CRA_a [Homo sapiens]	gi|119588290	90 kDa	2	2	0
neurochondrin isoform 2 [Homo sapiens]	gi|62526031	79 kDa	5	0	0
nuclear receptor coactivator 6 interacting protein, isoform CRA_b [Homo sapiens]	gi|119607168	97 kDa	13	0	0
7SK snRNA methylphosphate capping enzyme isoform A [Homo sapiens]	gi|47271406	74 kDa	13	0	0
RNA-binding protein 40 [Homo sapiens]	gi|40538732	59 kDa	13	0	0

Table S2: A selected dataset from the interactome analysis of SmN and SmB confirms efficient identification of known Sm protein interactors. All other core Sm family proteins were identified in the interactome analysis, as well as SMN, all Gemin components of the SMN complex and several LSm proteins, including LSm11 (found only in the U7 snRNP). Additionally, several members of the methylosome, where SmB post-translational modifications occur, were identified including Protein arginine N-methyltransferase 5 (PRMT5). Several previously identified SmB interactors (CD2 antigen cytoplasmic tail binding protein-2, PERQ2, WW domain-binding protein 4 and Formin binding protein 4) (Bedford et al. 1998, Bedford et al. 2000, Kofler et al. 2004, Kofler et al. 2005) were identified to interact with at least one of the proteins. * denotes that spectra from SmN were pooled with those from SmB by Scaffold due to sequence similarity in the majority of the proteins. Neurochondrin, and other proteins discussed are also shown here. Values are number of unique peptides identified.

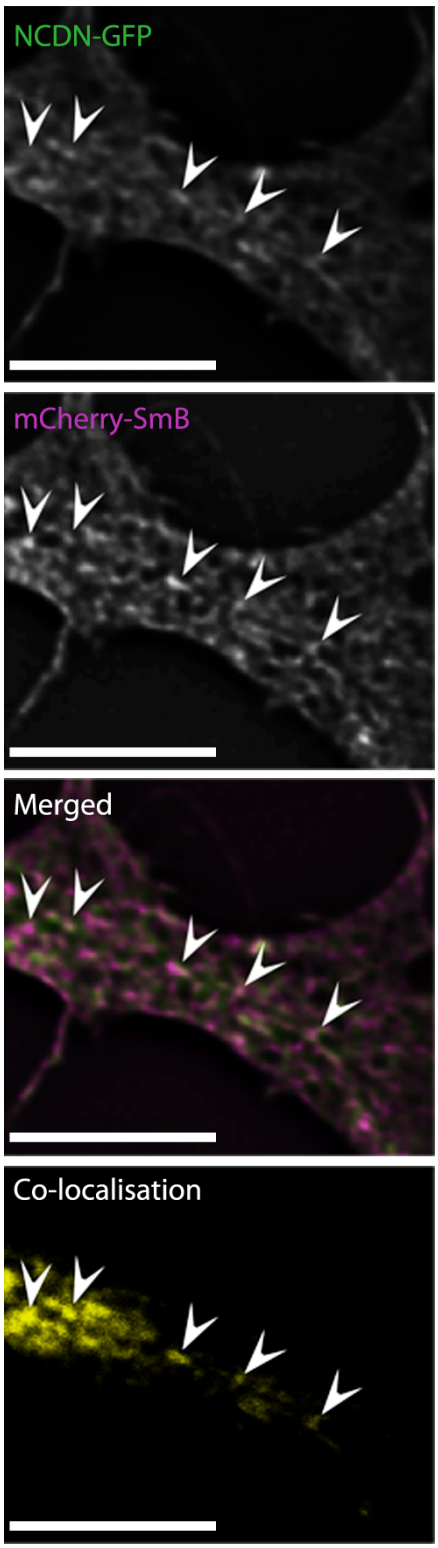

Figure S3: NCDN and SmB co-localise in neurites of SH-SY5Y cells constitutively expressing mCherry-SmB, and transiently expressing NCDN-GFP. Arrows identify SmB containing-vesicles with NCDN co-localisation. Bar= 7μm, images are single deconvolved z-sections. Co-localisation images were generated in Volocity, using automatic thresholds on non-deconvolved z-sections (see materials and methods).

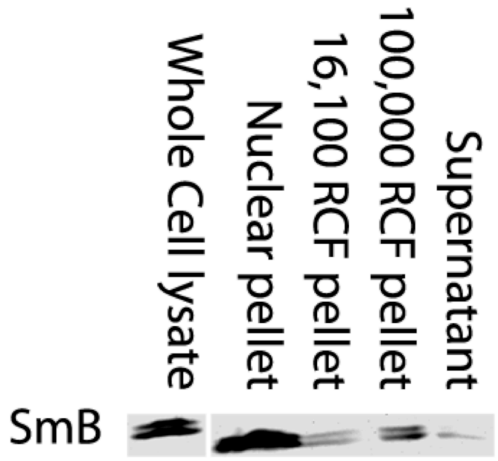

Figure S4: Endogenous SmB fractionates similarly to YFP-SmB and YFP-SmN, present in the 100,000 RCF vesicle fraction in and highly enriched in the nuclear pellet of fractionated SH-SY5Y cells. The gap between bands in the whole cell lysate and cell fractions signifies omitted lanes.

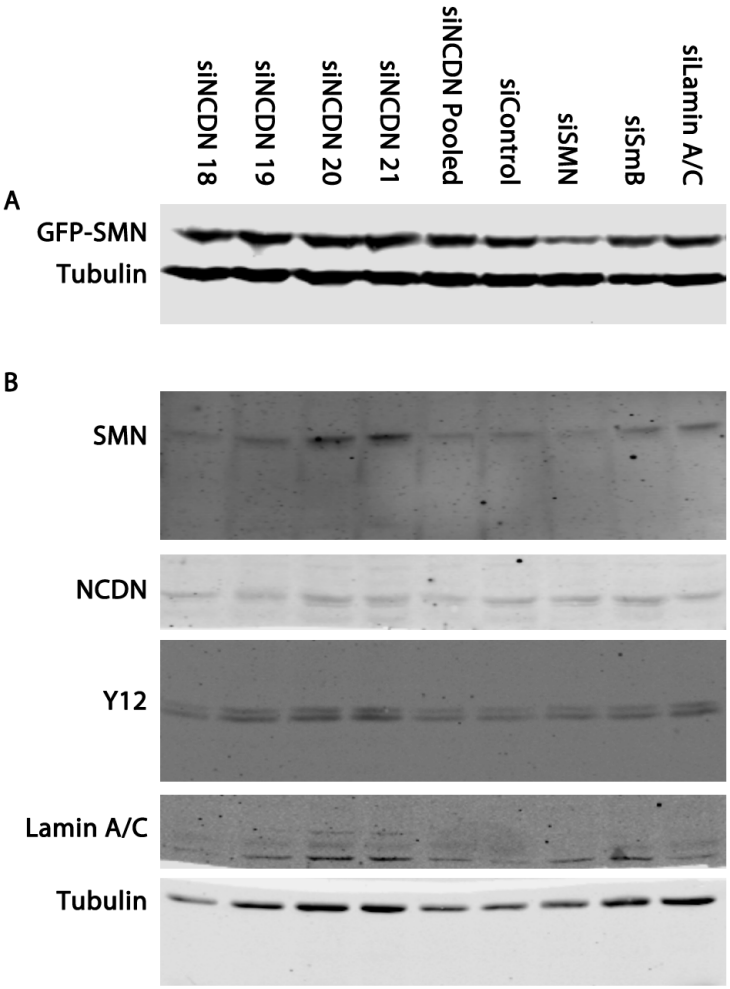

Figure S5: Quantified immunoblots of proteins targeted by siRNA in SH-SY5Y cells from Fig 5C. Equal volumes of lysate were immunoblotted, with band intensity of A) GFP-SMN, and B) SMN, NCDN, SmB (Y12) and lamin A/C quantified, and normalised to band intensity of tubulin, to determine the relative levels of protein expression.

Movie S1: punctate structures containing mCherry-SmN within the cytoplasm of SH-SH5Y cells are mobile. Images were taken every ~2 seconds for ~150 seconds. Movie is a projection of 3 deconvolved z-stacks taken with 0.5μm spacing. Bar=7μm.